INTERNATIONAL JOURNAL FOR NUMERICAL METHODS IN ENGINEERING, VOL. 2, 419–451 (1970)

ANALYSIS OF THICK AND THIN SHELL STRUCTURES BY CURVED FINITE ELEMENTS

SOHRABUDDIN AHMAD*

Civil Engineering Department, University of Engineering and Technology, Dacca, East Pakistan

BRUCE M. IRONS† AND O. C. ZIENKIEWICZ‡

Civil Engineering Department, University of Wales, Swansea

SUMMARY

A general formulation for the curved, arbitrary shape of thick shell finite elements is presented in this paper along with a simplified form for axisymmetric situations. A number of examples ranging from thin to thick shell applications are given, which include a cooling tower, water tanks, an idealized arch dam and an actual arch dam with deformable foundation.

A new process using curved, thick shell finite elements is developed overcoming the previous approximations to the geometry of the structure and the neglect of shear deformation.

A general formulation for a curved, arbitrary shape of shell is developed as well as a simplified form suitable for axisymmetric situations.

Several illustrated examples ranging from thin to thick shell applications are given to assess the accuracy of solution attainable. These examples include a cooling tower, tanks, and an idealized dam for which many alternative solutions were used.

The usefulness of the development in the context of arch dams, where a 'thick shell' situation exists, leads in practice to a fuller discussion of problems of foundation deformation, etc., so that practical application becomes possible and economical.

INTRODUCTION

The analysis of shells with an arbitrarily defined shape presents intractable analytical problems. If, in addition, the shell is a thick one in which shear deformation is significant the applicability of classical approaches become questionable. In civil engineering structures ranging from water tanks and cooling towers to pressure vessels and arch dams, these difficulties must be overcome if satisfactory (and hopefully optimized) designs are ever to be achieved.

Two paths are at present possible—structural models and numerical analysis by computer. Both present their own difficulties but clearly for design purposes the latter is more convenient.

In formulating numerical solutions to elastic shell problems many alternative approximations may be used. That of the finite element approach will be followed here.

In idealization of the shell by finite elements a geometrical simplification of replacing the curved shell by an assembly of flat elements is most frequently used.[1–3] With this simplification a large number of elements must invariably be used, and any advantage that can be gained by more sophisticated elements (which in smaller numbers can yield improved accuracy) is lost. Thus the need for elements which can take up curved shapes becomes obvious in this context.

---

* Formerly Commonwealth Research Scholar, Civil Engineering Department, University of Wales, Swansea.

† Lecturer.

‡ Professor of Civil Engineering and Head of the Department.

Received 1 October 1969

Some attempts to develop such curved shell elements have been made in recent years, but to date their application is limited to shallow shell situations and to those in which shear deformation is neglected.[4–7]

The development of large curvilinear elements for three-dimensional analysis by the relatively simple process of 'isoparametric' formulation (coupled with numerical integration) appears to open a possible avenue. Elements of the type shown in Figure 1 have for some years been used

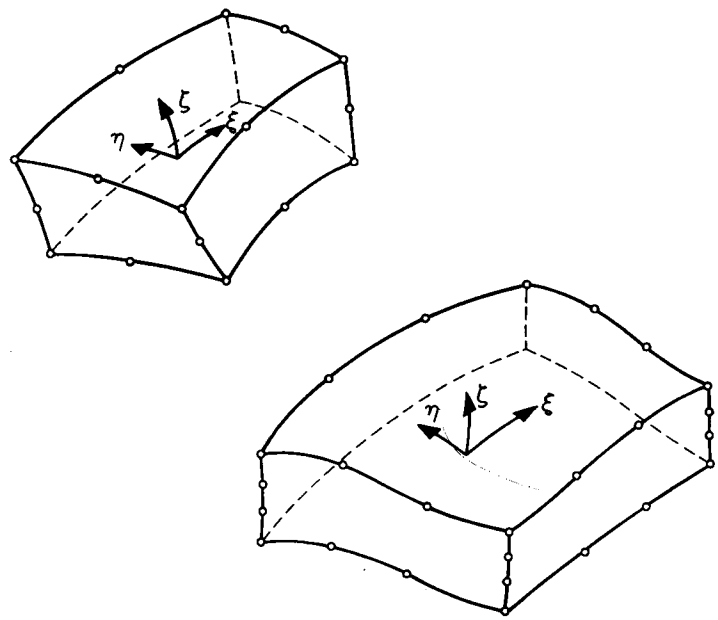

Figure 1. Three-dimensional hexahedral elements of parabolic and cubic types

with success for three-dimensional analysis purposes.[8–11] As the dimensions of such elements are completely arbitrary (and indeed are obtained simply by specifying nodal co-ordinates) one could visualize their 'attenuation' to represent geometrically a prescribed shell segment. Indeed such a representation would forcefully bring it home to the engineer that the classification of problems into shells, plates, etc. is an artificial one—introduced merely for the sake of convenience. Obviously in nature only three-dimensional problems exist and the sub-groups are introduced to reduce analytical or computational labour.

With a straightforward use of the three-dimensional concept, however, certain difficulties will be encountered.

In the first place the retention of three degrees of freedom at each node leads to large stiffness coefficients for relative displacements along an edge corresponding to the shell thickness. This presents numerical problems and inevitably leads to ill-conditioned equations when shell thicknesses become small compared with the other dimensions in the element.

The second factor is that of economy. The use of several nodes across the shell thickness ignores the well-known fact that even for thick shells the 'normals' to the middle surface remain practically straight after deformation. Thus an unnecessarily high number of degrees of freedom has to be carried, involving penalties of computer time.

In this paper a specialized formulation is presented overcoming both these difficulties.[12] The constraint of straight 'normals' is introduced to overcome the second problem and the strain

energy corresponding to stresses perpendicular to the middle surface is ignored. With these modifications an efficient tool for analysing curved thick shells becomes available. Its accuracy and wide range of applicability is demonstrated on several examples.

The reader will note that the two constraints introduced correspond only to a part of the usual assumptions of shell theory. Thus, the statement that after deformation the normals remain normal to the deformed middle surface has been deliberately omitted. This omission permits the shell to experience shear deformations—an important feature in thick shell situations.

Further, as integration is carried out numerically it is not necessary to introduce the various simplifying assumptions always present in conventional shell theory and resulting in the familiar situation of a wide variety of differential equations, apparently different, but describing the same problem. Indeed, in the very nature of the process, the need for formulating such equations disappears.

The paper is divided into three parts. The first is devoted to the description of the basic theory. While at this stage it is unnecessary to repeat the fundamentals of the 'displacement' approach to finite element theory, adequately given in a text,[1] it is felt essential to put on record some of the special mathematical manipulations needed to put the previously described assumptions into practice. It is hoped that this section will permit the suitably equipped reader to repeat and implement the computer programs used.

While the first part contains the 'meat' of the presentation the reader may proceed on cursory reading directly to the second and third parts presenting applications of the analysis. The second is concerned mainly with *verification* and outlines several examples of varying complexity for which solutions are available. The third deals in some detail with the special problems of arch dams—or indeed other similar shell structures in which foundation interaction is present.

THEORY

Geometric definition of the element

Consider the two typical thick shell elements of Figure 2(a). The external faces of the element are curved, while the sections across the thickness are generated by straight lines. Pairs of points, i_{top} and i_{bottom}, each with given Cartesian co-ordinates, prescribe the shape of the element.

Let ξ, η be two curvilinear co-ordinates in the middle plane of the shell and ζ a linear co-ordinate in the thickness direction. If further we assume that ξ, η, ζ vary between -1 and 1 on the respective faces of the element we can write a relationship between the Cartesian co-ordinates of any point of the shell and the curvilinear co-ordinates in the form

$$\begin{Bmatrix} x \\ y \\ z \end{Bmatrix} = \sum N_i(\xi,\eta)\frac{(1+\zeta)}{2}\begin{Bmatrix} x_i \\ y_i \\ z_i \end{Bmatrix}_{\text{top}} + \sum N_i(\xi,\eta)\frac{(1-\zeta)}{2}\begin{Bmatrix} x_i \\ y_i \\ z_i \end{Bmatrix}_{\text{bottom}} \tag{1}$$

Here $N_i(\xi,\eta)$ is a function taking a value of unity at the node i and zero at all other nodes. If the basic functions N_i are derived as 'shape functions' of a 'parent' element, square (or triangular) in plan (Figure 2b) and are so 'designed' that compatibility is achieved at interfaces, then the curved space elements will fit into each other. It is well known that for the first kind of element the functions are parabolic and for the second cubic in ξ and η and thus the curved shape of the shell element can take up a parabolic or cubic form respectively. By placing a larger number of nodes on the surfaces of the element more elaborate shapes can be achieved if so desired. Suitable shape functions for the elements of Figure 2(b) are listed in Appendix I.

The relation between the Cartesian and curvilinear co-ordinates is now established and it will be found desirable to operate with the curvilinear co-ordinates as the basis.

It should be noted that the co-ordinate direction ζ is *only approximately normal* to the middle surface.

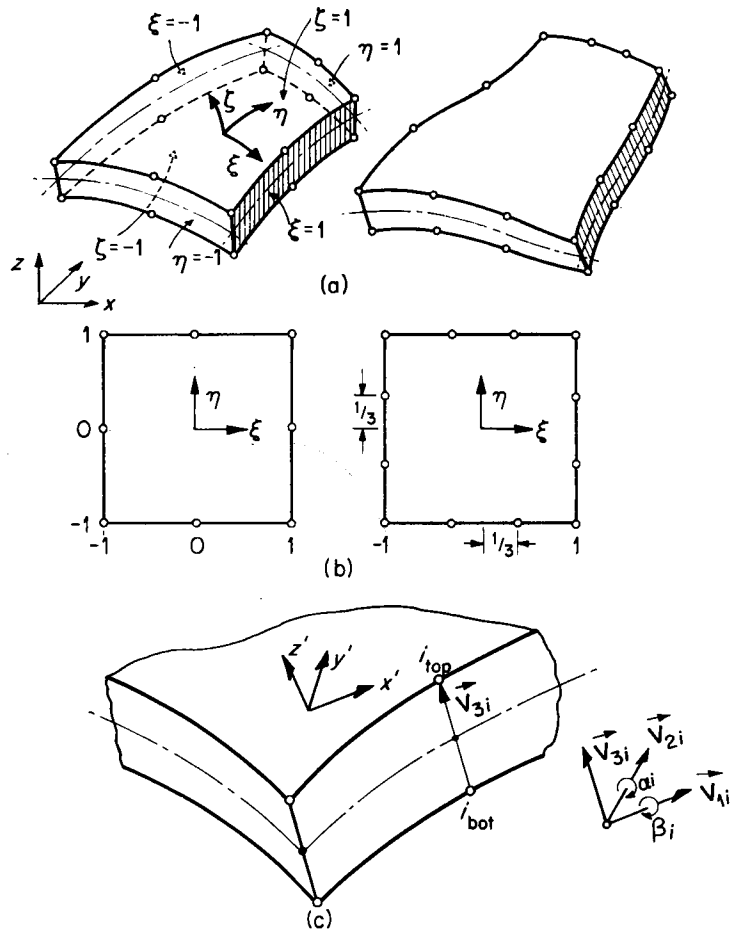

Figure 2. General curved shell elements; (a) Parabolic and cubic thick shell elements; (b) Parabolic and cubic 'parent' elements; (c) Geometry, local co-ordinates and nodal displacements

It is convenient to rewrite relationship (1) in a form specified by the 'vector' connecting the upper and lower points (i.e. a vector of length equal to the shell thickness t) and the mid-surface co-ordinates. Thus we have (Figure 2c)

$$\begin{Bmatrix} x \\ y \\ z \end{Bmatrix} = \sum N_i \begin{Bmatrix} x_i \\ y_i \\ z_i \end{Bmatrix}_{\text{mid}} + \sum N_i \frac{\zeta}{2} \vec{\mathbf{V}}_{3i} \tag{2}$$

with

$$\vec{\mathbf{V}}_{3i} = \begin{Bmatrix} x_i \\ y_i \\ z_i \end{Bmatrix}_{\text{top}} - \begin{Bmatrix} x_i \\ y_i \\ z_i \end{Bmatrix}_{\text{bottom}}$$

Displacement field

The displacement field has now to be specified for the element. As the strains in the direction normal to the mid-surface will be assumed to be negligible, the displacement throughout the element will be taken to be uniquely defined by the three Cartesian components of the mid-surface node displacement i and two rotations of the nodal vector $\vec{\mathbf{V}}_{3i}$ about orthogonal directions normal to it. If two such orthogonal directions are given by vectors $\hat{\mathbf{v}}_{2i}$ and $\hat{\mathbf{v}}_{1i}$ (of unit magnitude) with corresponding (scalar) rotations α_i and β_i we can write, dropping the suffix 'mid' of equation (2):

$$\begin{Bmatrix} u \\ v \\ w \end{Bmatrix} = \sum N_i \begin{Bmatrix} u_i \\ v_i \\ w_i \end{Bmatrix} + \sum N_i \zeta \frac{t_i}{2} [\hat{\mathbf{v}}_{1i}, -\hat{\mathbf{v}}_{2i}] \begin{Bmatrix} \alpha_i \\ \beta_i \end{Bmatrix} \tag{3}$$

where u, v and w are displacements in the directions of the global x, y and z axes.

As an infinity of vector directions normal to a given direction can be generated, a particular scheme has been devised to ensure a *unique* definition. This is given in Appendix II.

Once again if N_i are compatible functions then displacement compatibility is maintained between adjacent elements.

It can also be shown that the displacement definition reproduces any state of rigid body motion—a condition necessary for convergence.*[1,10]

Physically, it has been assumed in the definition of equation (3) that no strains occur in the direction ζ. While this is not exactly normal to the middle surface it represents to a good approximation one of the usual shell assumptions.

At each node i of Figure 2(c) we have now the five basic degrees of freedom.

Definition of strains and stresses

To derive the basic properties of a finite element the essential strains and stresses have to be defined.[1] The components in directions of orthogonal axes related to the surface ζ = constant are essential if account is to be taken of the basic shell assumptions. Thus if at a point in this surface we erect a normal z' with two other orthogonal axes x' and y' tangent to it (Figure 2c) the strain components of interest are

$$\{\boldsymbol{\varepsilon}'\} = \begin{Bmatrix} \varepsilon_{x'} \\ \varepsilon_{y'} \\ \gamma_{x'y'} \\ \gamma_{x'z'} \\ \gamma_{y'z'} \end{Bmatrix} = \begin{Bmatrix} \dfrac{\partial u'}{\partial x'} \\ \dfrac{\partial v'}{\partial y'} \\ \dfrac{\partial u'}{\partial y'} + \dfrac{\partial v'}{\partial x'} \\ \dfrac{\partial w'}{\partial x'} + \dfrac{\partial u'}{\partial z'} \\ \dfrac{\partial w'}{\partial y'} + \dfrac{\partial v'}{\partial z'} \end{Bmatrix} \tag{4}$$

with the strain in direction z' neglected so as to be consistent with the shell assumption. It must be noted that in general none of these directions coincide with those of the curvilinear co-ordinates ξ, η, ζ, although x', y' are in the ξ–η plane (ζ = constant).

* As the definition of the co-ordinates is more general than that of the displacements but includes it as a special case the elements are called *superparametric*, to distinguish from the isoparametric elements of References 8–11.

The stresses corresponding to these strains are defined by a matrix $\{\sigma'\}$ and are related by the elasticity matrix $[\mathbf{D}']$. Thus

$$\{\sigma'\} = \begin{Bmatrix} \sigma_{x'} \\ \sigma_{y'} \\ \tau_{x'y'} \\ \tau_{x'z'} \\ \tau_{y'z'} \end{Bmatrix} = [\mathbf{D}'](\{\varepsilon'\} - \{\varepsilon_0'\}) \tag{5}$$

where $\{\varepsilon_0'\}$ may represent any 'initial' strains due, for instance, to thermal expansion.

The 5×5 matrix $[\mathbf{D}']$ can now include any anisotropic properties and indeed may be prescribed as a function of ζ if sandwich construction is used. For the present moment we shall define it only for an isotropic material. Here

$$[\mathbf{D}'] = \frac{E}{(1-\nu^2)} \begin{bmatrix} 1 & \nu & 0 & 0 & 0 \\ & 1 & 0 & 0 & 0 \\ & & \frac{1-\nu}{\nu} & 0 & 0 \\ & & & \frac{1-\nu}{2k} & 0 \\ & \text{sym.} & & & \frac{1-\nu}{2k} \end{bmatrix} \tag{6}$$

in which E and ν are Young's modulus and Poisson's ratio respectively. The factor k included in the last two shear terms is taken as 1·2 and its purpose is to improve the shear displacement approximation. From the displacement definition it will be seen that the shear distribution is approximately constant through the thickness, whereas in reality the shear distribution is approximately parabolic. The value $k = 1{\cdot}2$ is the ratio of relevant strain energies.

Element properties and necessary transformations

The stiffness matrix—and indeed all other 'element' property matrices—involves integrals over the volume of the element, which are quite generally of the form

$$\int_{\text{vol.}} [\mathbf{S}]\, dx\, dy\, dz \tag{7}$$

where the matrix $[\mathbf{S}]$ is a function of the co-ordinates.

In the stiffness matrix

$$[\mathbf{S}] = [\mathbf{B}]^{\mathrm{T}}[\mathbf{D}][\mathbf{B}] \tag{8}$$

for instance, with the definition

$$\{\varepsilon\} = [\mathbf{B}]\{\delta\}^{\mathrm{e}} \tag{9}$$

so that $[\mathbf{B}]$ relates the strains to the nodal parameters. The theory of the subject is given in the text[1] and many other references, and need not be dwelt upon here.

If in the present context we can express $[\mathbf{S}]$ as an explicit function of the curvilinear co-ordinates and transform similarly the infinitesimal volume, $dx\,dy\,dz$, then a straightforward (numerical) integration will allow the properties to be evaluated. Thus some transformations are necessary.

Equation (3) relates the global displacements u, v, w to the curvilinear co-ordinates.

The derivatives of these displacements with respect to the global x, y, z co-ordinates are given by a matrix relation

$$\begin{bmatrix} \frac{\partial u}{\partial x} & \frac{\partial v}{\partial x} & \frac{\partial w}{\partial x} \\ \frac{\partial u}{\partial y} & \frac{\partial v}{\partial y} & \frac{\partial w}{\partial y} \\ \frac{\partial u}{\partial z} & \frac{\partial v}{\partial x} & \frac{\partial w}{\partial z} \end{bmatrix} = [\mathbf{J}]^{-1} \begin{bmatrix} \frac{\partial u}{\partial \xi} & \frac{\partial v}{\partial \xi} & \frac{\partial w}{\partial \xi} \\ \frac{\partial u}{\partial \eta} & \frac{\partial v}{\partial \eta} & \frac{\partial w}{\partial \eta} \\ \frac{\partial u}{\partial \zeta} & \frac{\partial v}{\partial \zeta} & \frac{\partial w}{\partial \zeta} \end{bmatrix} \tag{10}$$

The Jacobian matrix is defined as

$$[\mathbf{J}] = \begin{bmatrix} \frac{\partial x}{\partial \xi} & \frac{\partial y}{\partial \xi} & \frac{\partial z}{\partial \xi} \\ \frac{\partial x}{\partial \eta} & \frac{\partial y}{\partial \eta} & \frac{\partial z}{\partial \eta} \\ \frac{\partial x}{\partial \zeta} & \frac{\partial y}{\partial \zeta} & \frac{\partial z}{\partial \zeta} \end{bmatrix} \tag{11}$$

and is calculated from the co-ordinate definition of equation (2).

Now, for every set of curvilinear co-ordinates the global displacement derivatives can be obtained numerically. A further transformation to local displacement directions x', y', z' will allow the strains, and hence the **[B]** matrix, to be evaluated.

First the directions of the local axes have to be established. A vector normal to the surface ζ = constant can be found as a vector product of any two vectors tangent to the surface. Thus

$$\vec{\mathbf{V}}_3 = \begin{Bmatrix} \frac{\partial x}{\partial \xi} \\ \frac{\partial y}{\partial \xi} \\ \frac{\partial z}{\partial \xi} \end{Bmatrix} \times \begin{Bmatrix} \frac{\partial x}{\partial \eta} \\ \frac{\partial y}{\partial \eta} \\ \frac{\partial z}{\partial \eta} \end{Bmatrix} = \begin{Bmatrix} \frac{\partial y}{\partial \xi}\frac{\partial z}{\partial \eta} - \frac{\partial y}{\partial \eta}\frac{\partial z}{\partial \xi} \\ \frac{\partial x}{\partial \eta}\frac{\partial z}{\partial \xi} - \frac{\partial x}{\partial \xi}\frac{\partial z}{\partial \eta} \\ \frac{\partial x}{\partial \xi}\frac{\partial y}{\partial \eta} - \frac{\partial x}{\partial \eta}\frac{\partial y}{\partial \xi} \end{Bmatrix} \tag{12}$$

Following the process which defines uniquely two perpendicular vectors, as given in Appendix II, and reducing to unit magnitudes, we construct a matrix of unit vectors in x', y', z' directions (which is in fact the direction cosine matrix)

$$[\theta] = [\hat{\mathbf{v}}_1, \hat{\mathbf{v}}_2, \hat{\mathbf{v}}_3] \tag{13}$$

The global derivatives of displacements u, v and w are now transformed to the local derivatives of the local orthogonal displacements by a standard operation

$$\begin{bmatrix} \frac{\partial u'}{\partial x'} & \frac{\partial v'}{\partial x'} & \frac{\partial w'}{\partial x'} \\ \frac{\partial u'}{\partial y'} & \frac{\partial v'}{\partial y'} & \frac{\partial w'}{\partial y'} \\ \frac{\partial u'}{\partial z'} & \frac{\partial v'}{\partial z'} & \frac{\partial w'}{\partial z'} \end{bmatrix} = [\boldsymbol{\theta}]^{\mathrm{T}} \begin{bmatrix} \frac{\partial u}{\partial x} & \frac{\partial v}{\partial x} & \frac{\partial w}{\partial x} \\ \frac{\partial u}{\partial y} & \frac{\partial v}{\partial y} & \frac{\partial w}{\partial y} \\ \frac{\partial u}{\partial z} & \frac{\partial v}{\partial z} & \frac{\partial w}{\partial z} \end{bmatrix} [\boldsymbol{\theta}] \tag{14}$$

From this the components of the [B′] matrix can now be found explicitly

$$\{\varepsilon'\} = [\mathbf{B}'] \begin{Bmatrix} \{\delta_1\} \\ \{\delta_2\} \\ \vdots \\ \{\delta_j\} \end{Bmatrix}; \quad \{\delta_i\} = \begin{Bmatrix} u_i \\ v_i \\ w_i \\ \alpha_i \\ \beta_i \end{Bmatrix} \tag{15}$$

The infinitesimal volume is given in terms of the curvilinear co-ordinates as

$$\mathrm{d}x\,\mathrm{d}y\,\mathrm{d}z = \text{determinant } [\mathbf{J}]\,\mathrm{d}\xi\,\mathrm{d}\eta\,\mathrm{d}\zeta \tag{16}$$

and this standard expression completes the basic formulation.

The computer programs use Gaussian quadrature for the integration. The two-point rule suffices in the ζ direction, while a minimum of three or four points in both ξ and η directions is needed for parabolic or cubic elements respectively.

Some remarks on solution

The element properties are now defined, and the assembly and solution are standard processes. A particularly effective scheme of equation-solving known as the 'front solution' is used because it is inherently better than a banded solution for elements containing mid-side nodes.[13]

It remains to discuss the presentation of the stresses, and this problem is of some consequence. The strains being defined in local directions, $\{\sigma'\}$ is readily available. These are indeed directly of interest but as the directions of local axes are not easily visualized it is convenient to transfer the components to the global system using the following expression

$$\begin{bmatrix} \sigma_x & \tau_{xy} & \tau_{xz} \\ \tau_{xy} & \sigma_y & \tau_{yz} \\ \tau_{xz} & \tau_{yz} & \sigma_z \end{bmatrix} = [\theta] \begin{bmatrix} \sigma_{x'} & \tau_{x'y'} & \tau_{x'z'} \\ \tau_{x'y'} & \sigma_{y'} & \tau_{y'z'} \\ \tau_{x'z'} & \tau_{y'z'} & 0 \end{bmatrix} [\theta]^{\mathrm{T}} \tag{17}$$

If the stresses are calculated at a nodal point where several elements meet then they are averaged.

In a general shell structure, such as a doubly curved arch dam, the stresses in a global system do not, however, give a clear picture of shell surface stresses. The matrix–vector handling scheme[14] (developed for convenience in dealing with the various transformations—see Appendix III) therefore includes a 'Jacobi' eigenvalue routine which diagonalizes the stress tensor giving the principal stresses. The direction cosines of such stresses are obtained as vectors.

Regarding the shell surface stresses more rationally, one may note that the shear components $\tau_{x'z'}$ and $\tau_{y'z'}$ are in fact zero there, and can indeed be made zero at the stage before converting to global components. The values directly obtained for these shear components are the average values across the section. The maximum transverse shear value occurs on the neutral axis and is equal to 1·5 times the average value.

'VERIFICATION' AND GENERAL EXAMPLES

General remarks

Most numerical processes are by their very nature approximate, because of curtailment of significant digits (round-off) or various physical idealizations introduced into the process of solution. An assessment of accuracy attainable with the present computational scheme, therefore,

needs to be made. In this section a series of examples ranging from thin to thick shell situations will be presented to demonstrate the accuracy attainable and hence the limitations of the solution.

Several special classes of problems will be discussed.

Axi-symmetric shell with axi-symmetric load

If the geometry of the shell is that of a body of revolution and in addition the loading is symmetric about the axis, the general program can be simplified considerably. Only two co-ordinates are now necessary to define the geometry of a particular point and the degrees of freedom at a typical node reduce to three instead of five. Details of such modifications are fully described in Reference 12 and need not be repeated here.

Several examples in this class of problem will be given.

Example 1

Spherical dome under uniform pressure, Figure 3. An 'exact' solution based on thin shell theory[15] is known for this simple case. In Figure 3 a comparison of moments and hoop forces is given for a subdivision using 24 cubic elements. The size of elements is graded, the smallest being used in the vicinity of the encastré end.

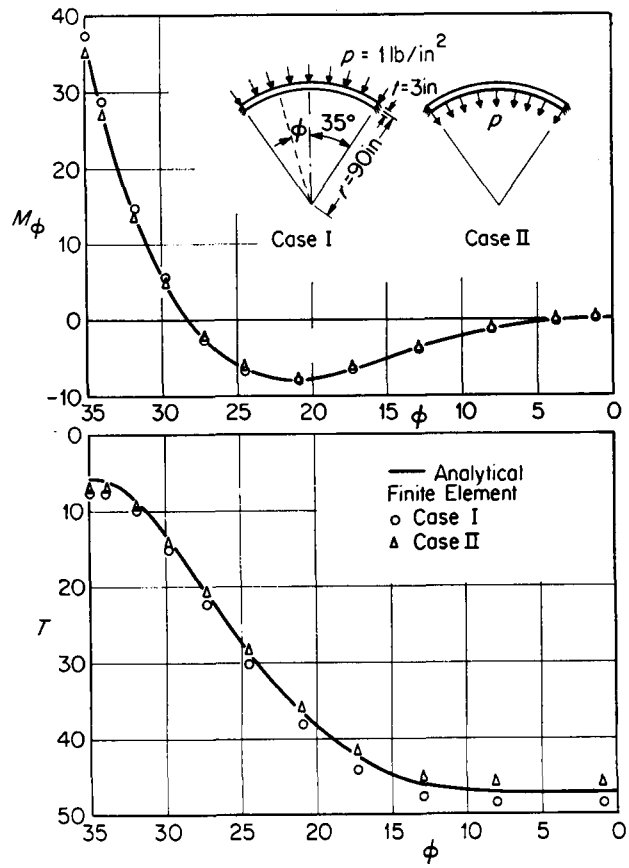

Figure 3. Spherical dome under uniform pressure analysed with 24 elements. (First element subtends an angle of 0·1° from the fixed end, others in arithmetic progression.) M_ϕ = Meridional bending moment in.-lb/in.; T = Hoop force lb/in.; $\nu = \frac{1}{8}$

When the shell is thin, negligible shear effects are expected, but the differences obtained due to applying the pressure at inner and outer surfaces are worth noting. (The conventional thin shell theory applies to all loads at the middle surface.)

The accuracy obtained is excellent.

Example 2

Thin cylinder under radial edge load, Figure 4. Again a theoretical solution is available, which has been used extensively as a 'test' for other finite element solutions.[16,17] Here it was chosen because of its extreme thinness. Also the effects of various subdivisions into cubic type elements

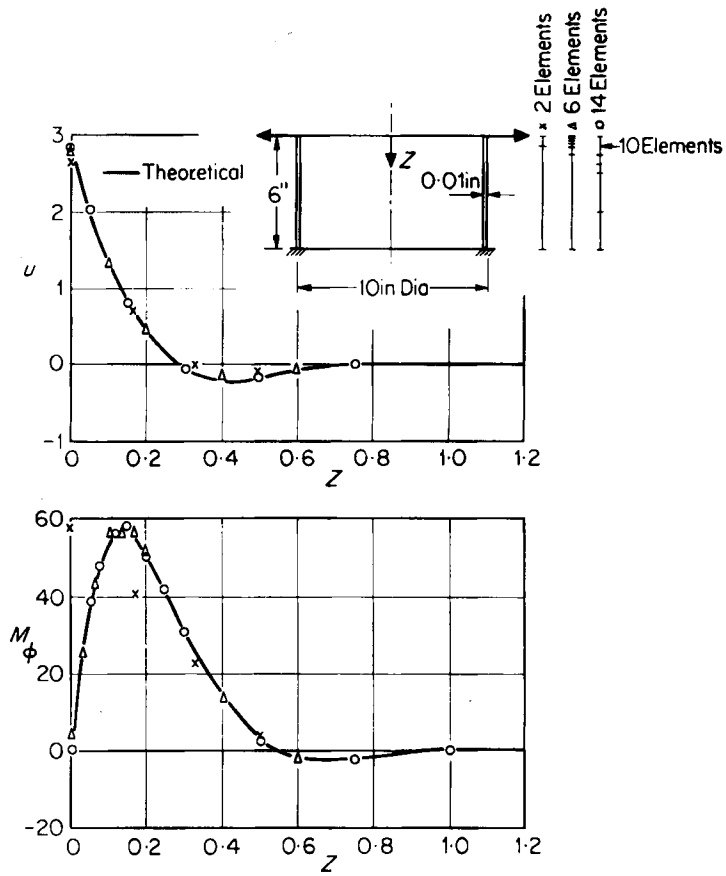

Figure 4. Thin cylinder under radial edge load. u = Radial displacement, in. $\times 10^{-3}$; M_ϕ = Meridional moment, in.-lb/in. $\times 10^{-3}$; $E = 10^7$ lb/in.^{2}; $\nu = 0{\cdot}3$

could be studied. It will be observed that even with as few as two elements reasonable deflections are obtained, although clearly the rapid moment variation at the ends is only crudely approximated.

Example 3

A thick water-retaining tank, Figure 5. This problem, in which thick and thin sections occur simultaneously, is clearly outside the range of theoretical solutions. Here the basis of comparison

is a fully two-dimensional solution obtained by the finite element process.[18] With 15 cubic elements in each case the agreement between the two solutions is remarkably good, but the computer times were in the ratio 1 : 3, so that the shell solution is much cheaper.

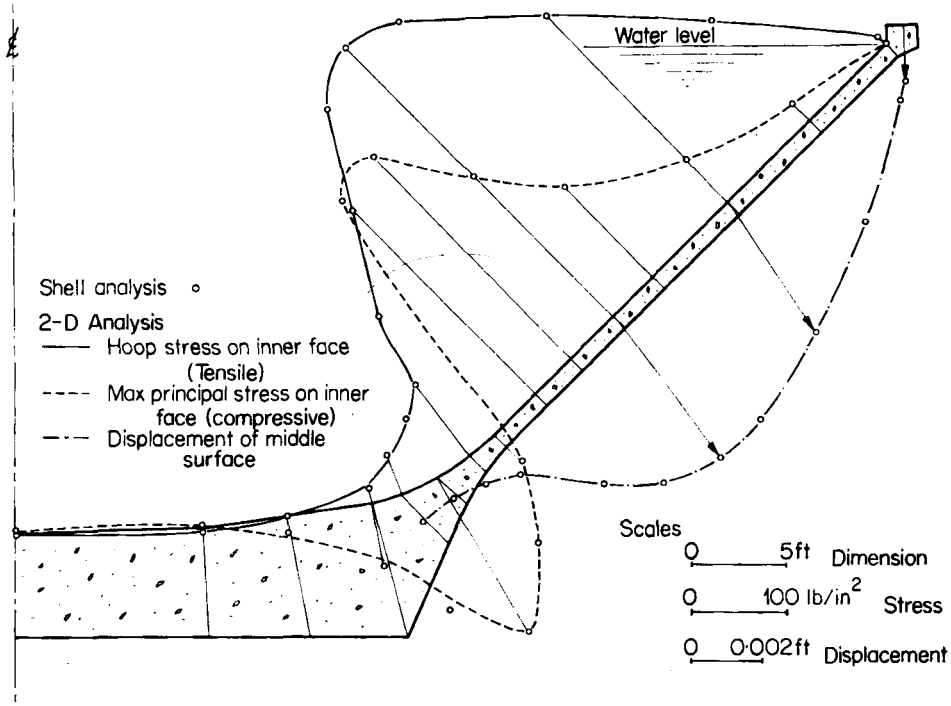

Figure 5. A thick water-retaining tank, $E = 5 \times 10^6$ lb/in.^{2}; $\nu = 0{\cdot}2$

The results show clearly the effectiveness of the new shell program in problems which would not normally be described as 'shells'.

Axi-symmetric shells with non-symmetric load

Even if the load on an axi-symmetric shell is not symmetric, it can always be described in terms of its harmonic components. In such cases one can retain the simplicity of axi-symmetric formulation and still use an element subdivision in a cross-section only. The analysis for each harmonic component of load is carried out separately because their effects in an elastic case are 'uncoupled'. The basic theory is already well known and is not repeated here.[12,16] An example which applies to the present element in this manner is given in Reference 12. However, two additional examples of civil engineering interest are presented here for completeness.

Example 4

Cooling tower under wind load, Figures 6–9. The subject of cooling tower design and analysis is of some interest to the profession and recently many papers have appeared on the subject. The details of the present example (Figure 6) are taken from a paper by Albasiny and Martin[19] who developed a special process for dealing with this problem. Figures 7–9 show that the results obtained by using 15 cubic elements are indistinguishable from those of Reference 19.

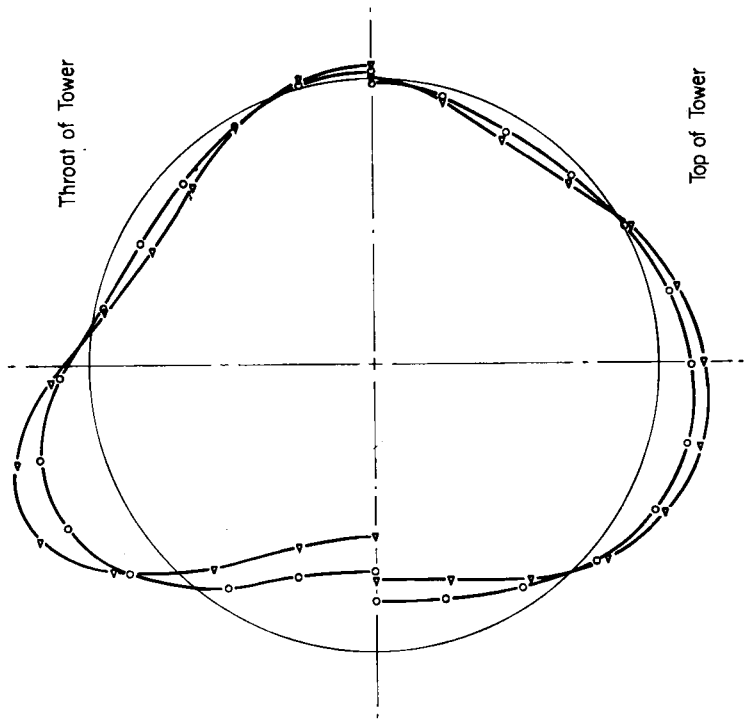

Figure 7. Distortion of horizontal sections at throat and top

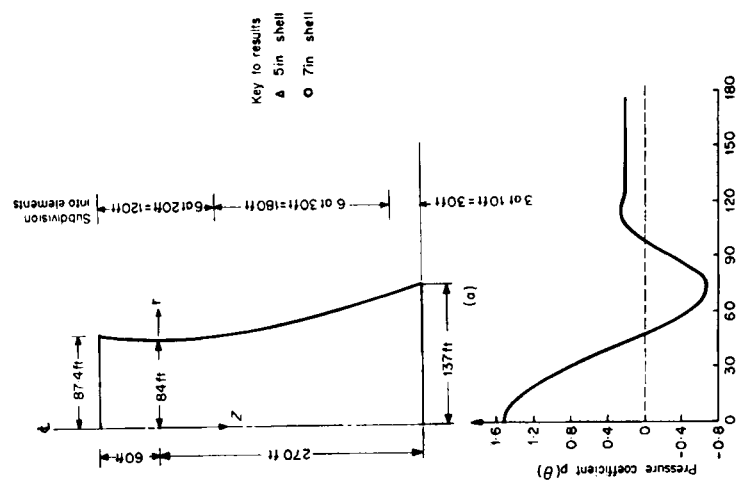

Figure 6. Cooling tower under wind load; (a) Geometry of specimen cooling tower. $E = 3 \times 10^6 \text{lb/in}^2$; $\nu = 0{\cdot}15$; (b) Wind pressure distributions used in the calculations

Example 5

'Hill-side' water tank, Figures 10–12. This further civil engineering example is included to show an application to the frequently encountered situation of a tank subject to unsymmetric earth pressure loads.

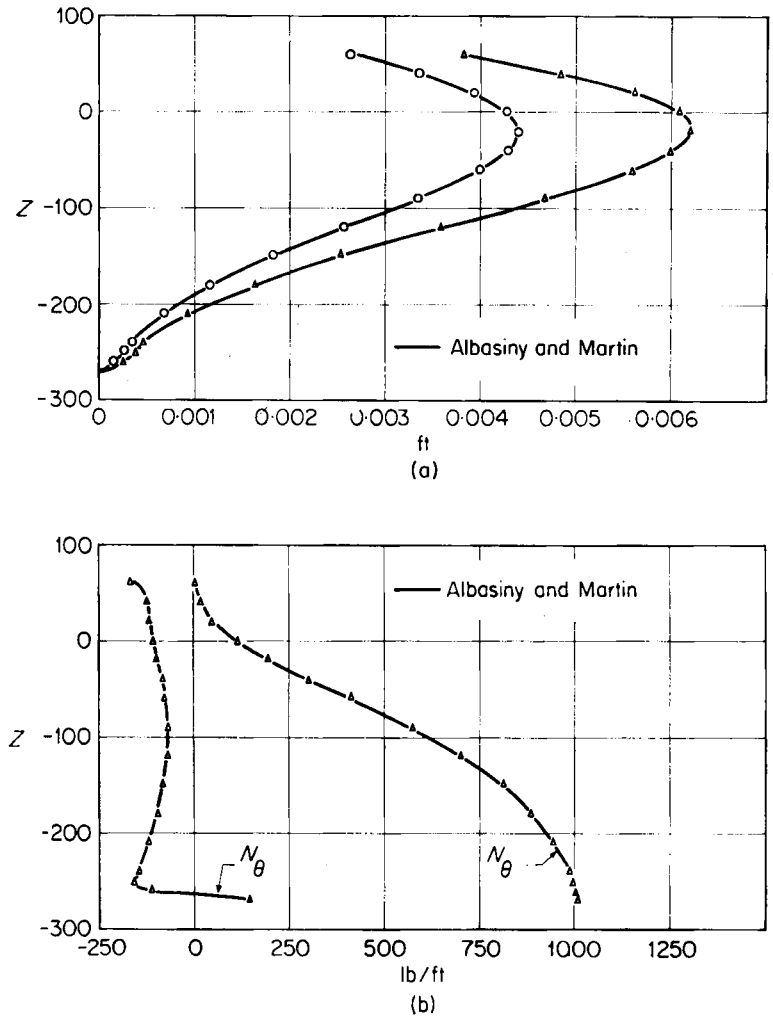

Figure 8. (a) Distribution of radial displacements with height at $\theta = 0°$; (b) Distribution of membrane forces with height at $\theta = 0°$. N_ϕ = Meridional membrane force; N_θ = Tangential membrane force

For convenience the non-uniform earth pressure is idealized as two hydrostatic pressures forming a single step. The difference between them (say p) over the quadrant ($-45° < \theta < 45°$) is then represented with six harmonics (Figure 10). The coefficients p_n of the relation $p = \sum p_n \cos n\theta$ are given in Table I.

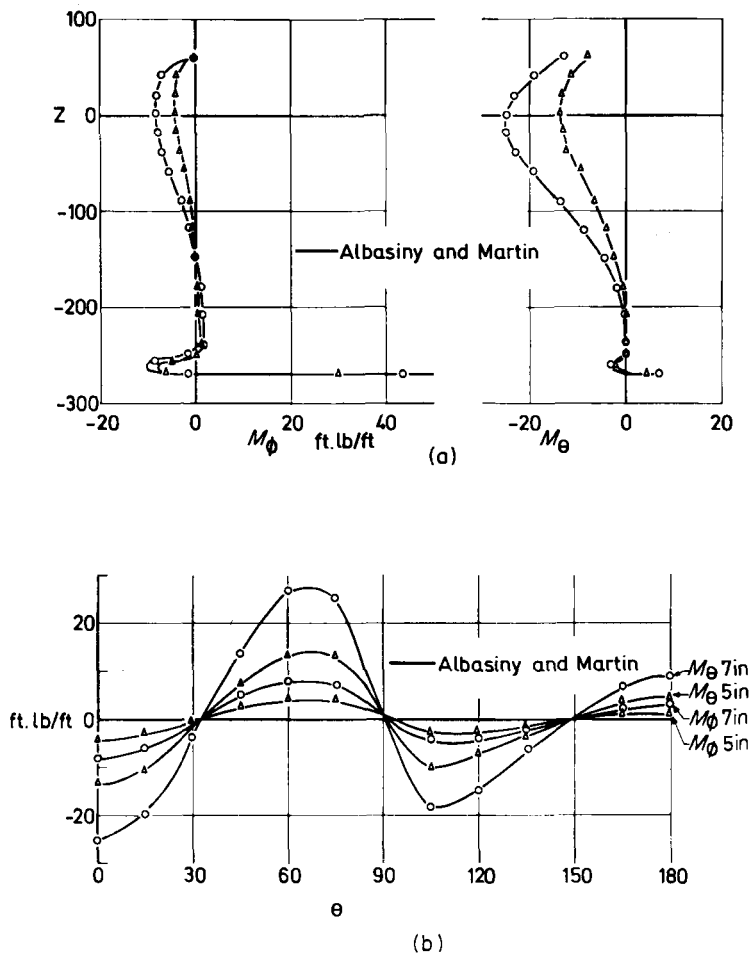

Figure 9. (a) Distribution of bending moments with height at $\theta = 0°$; (b) Distribution of bending moment at $z = 0$. M_ϕ = Meridional bending moment; M_θ = Tangential bending moment

Table I. Pressure coefficients

n	p_n	n	p_n
0	$+0{\cdot}2500p$	3	$+0{\cdot}1500p$
1	$+0{\cdot}4501p$	5	$-0{\cdot}0900p$
2	$+0{\cdot}3183p$	6	$-0{\cdot}1061p$

The action of internal water pressure and roof loading are also included in the analysis as they involve very little extra effort.

Figure 11(a) shows the distortion of the vertical section for all the loadings. The earth pressure being unsymmetric the displacements as well as direct forces and moments vary in the θ direction as shown in Figures 11(b) and 11(c). The distribution of meridional moments and tangential forces along the vertical section are shown in Figures 12(a) and 12(b).

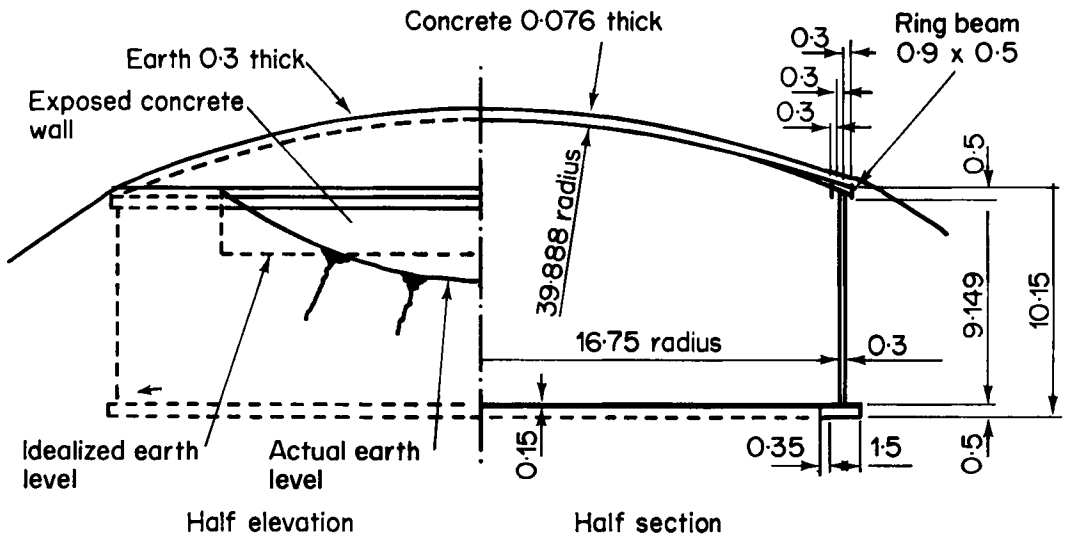

(a)

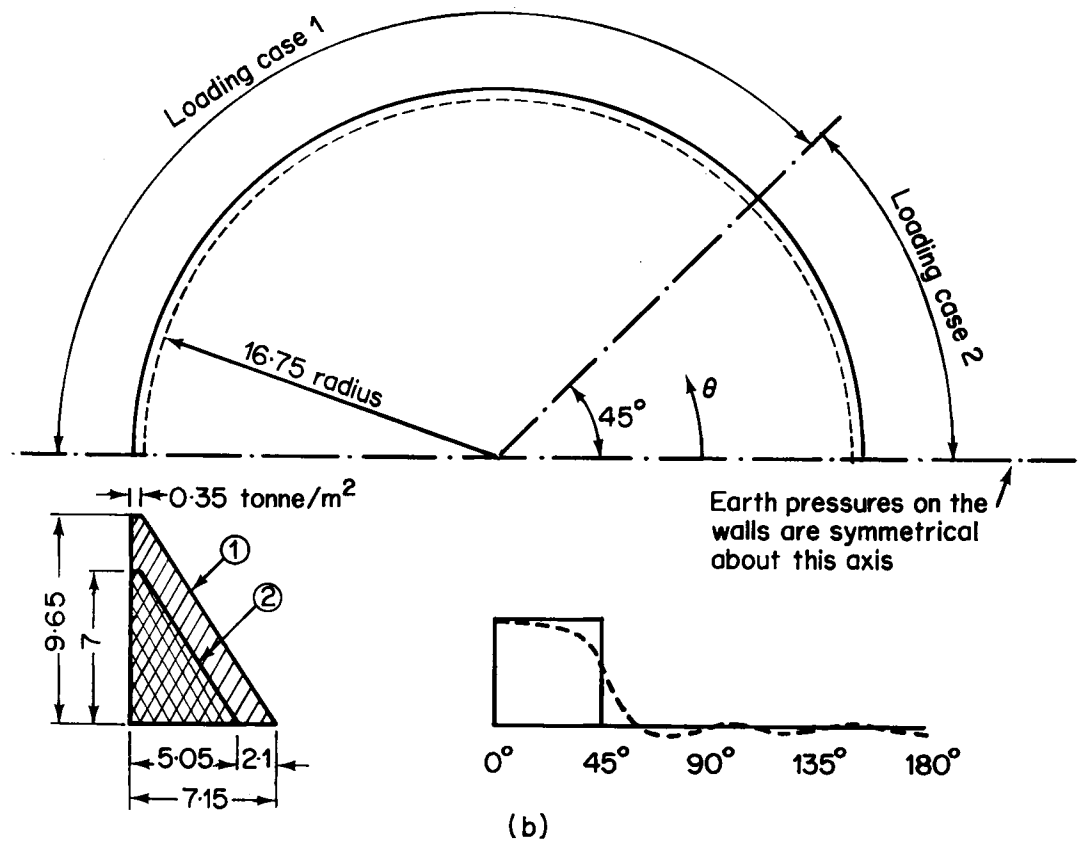

(b)

Figure 10. Hillside water tank; (a) Elevation and section of tank. Dimension in meters: $E = 5 \times 10^6$ lb/in.^{2}; $\nu = 0{\cdot}15$; (b) Idealized distribution of earth pressure

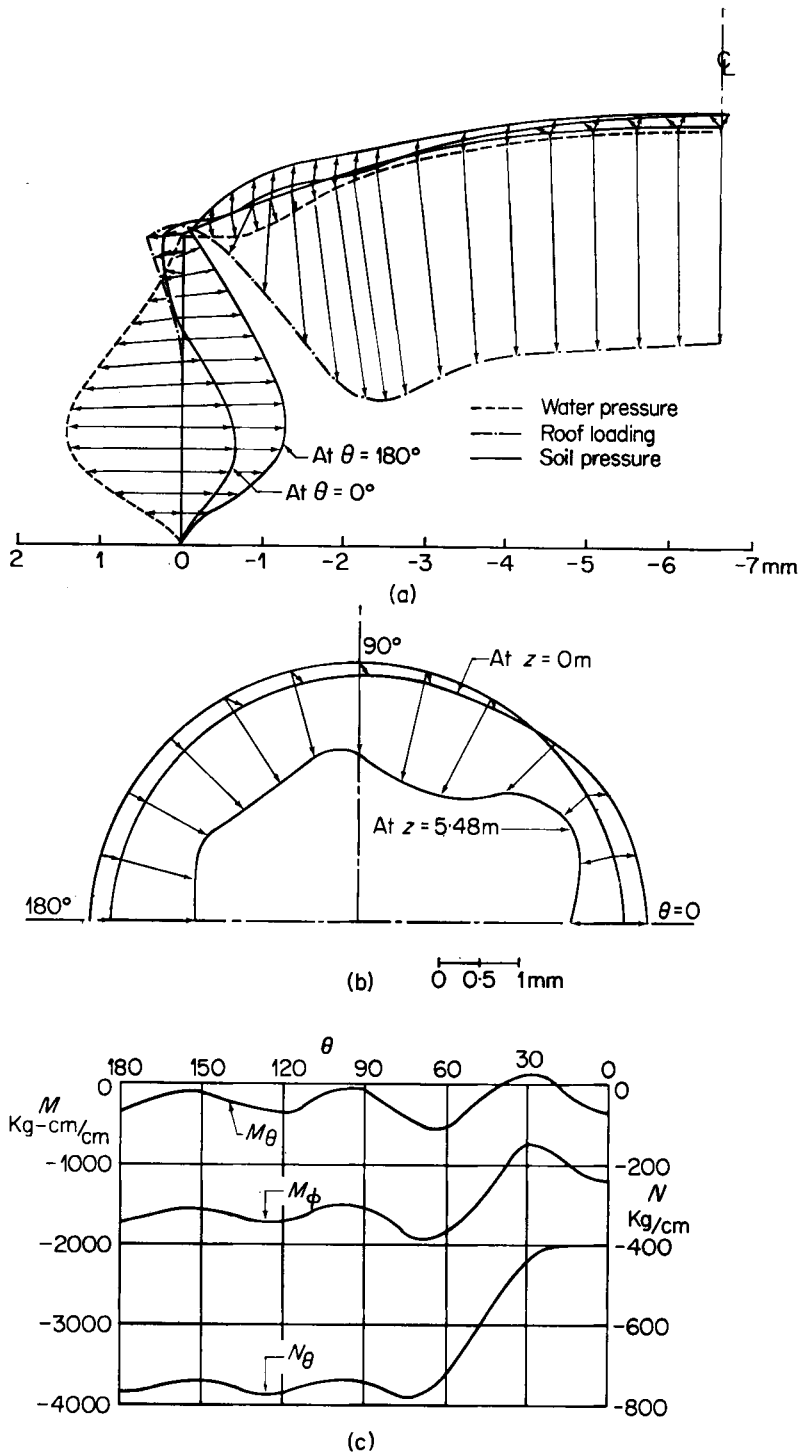

Figure 11. (a) Distortion of vertical section at $\theta = 0°$ and $\theta = 180°$; (b) Distortion of horizontal section at $z = 5{\cdot}48$ m (soil pressure only); (c) Distribution of N_θ, M_θ and M_ϕ at $z = 5{\cdot}48$ m. N_θ = Tangential force; M_θ = Tangential moment; M_ϕ = Meridional moment

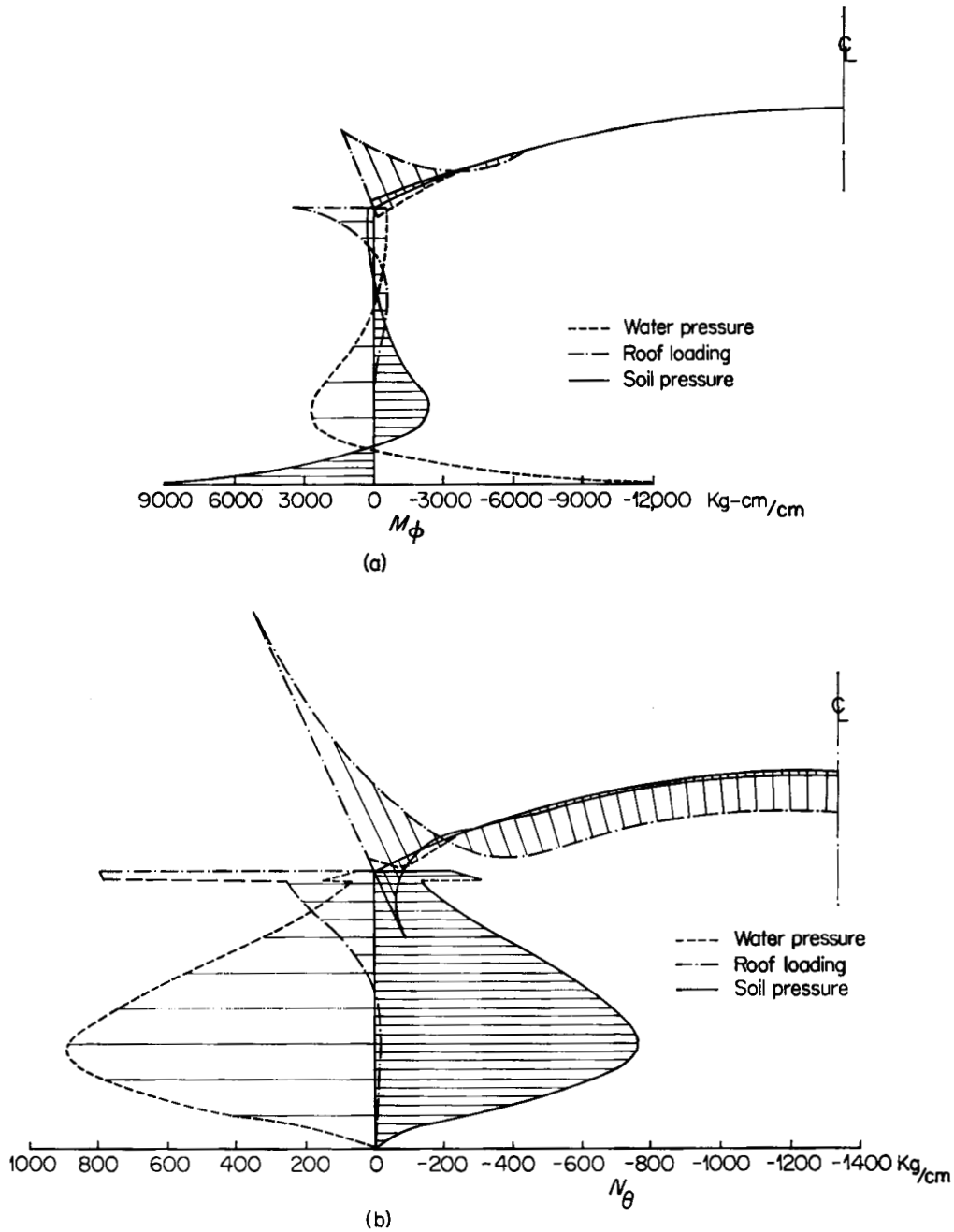

Figure 12. (a) Distribution of meridional moment (M_ϕ) with height at $\theta = 180°$; (b) Distribution of tangential force (N_θ) with height at $\theta = 180°$

Flat plates

The formulation is a general one and must obviously be capable of dealing with the problem of plates. Indeed in this special case the 'in plane' degrees of freedom can be suppressed and there are only three degrees of freedom at a node.

Therefore a general plate element is now available which can represent to a good approximation the action of *thick* plates without introducing complex theories such as those due to Reissner.[20] Such an element is invaluable in the solution of *bridge slab* problems when their proportions are such that thin plate theory is no longer applicable. For most such problems the standard solutions use thin plate theory at the present time.[21]

Example 6

Circular plate, Figure 13. Thick and thin plate solutions are available here from the work of Timoshenko.[22] With double symmetry only a quarter of the plate need be analysed, and the mesh

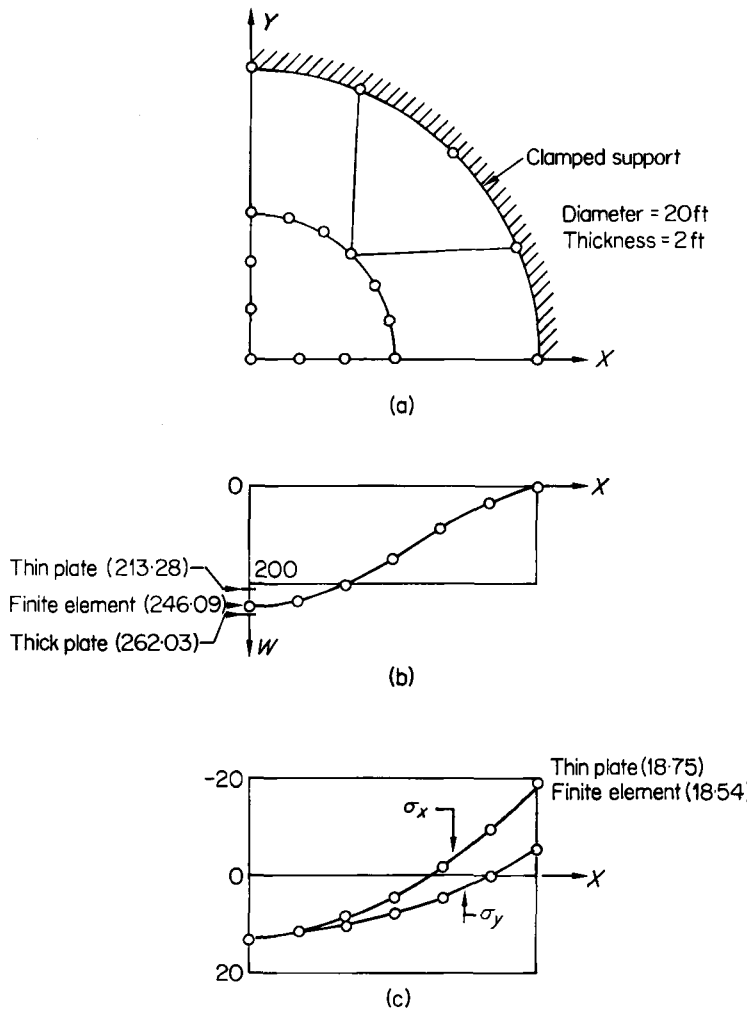

Figure 13. Circular plate under uniformly distributed load, $\nu = 0{\cdot}3$; (a) Subdivision into four cubic elements; (b) Distribution of vertical displacement along a radius; (c) Distribution of stresses along a radius. σ_x = Radial bending stress; σ_y = Tangential bending stress

of four cubic elements is shown in Figure 13(a). Deflections and bending stresses are compared in Figures 13(b) and 13(c). For a thickness/diameter ratio of 0·1 the maximum deflection obtained even with this coarse mesh is as much as 16 per cent higher than that calculated from the thin plate assumption; the theoretical value with thick plate solution assumptions is 23 per cent higher.

This example also shows the remarkable versatility of the elements in following curved boundaries.

Arbitrarily shaped shells

Although the method of computation outlined was originally aimed at this general class of problems, this section is presented last because few general solutions are available against which examples can be tested.

Example 7

Long cylindrical shell (ring) under gravity action with line support, Figure 14. This example is almost trivial, as it can be solved by simple bending theory. Here, it is solved using eight parabolic elements, and Figure 14 shows the close agreement of the results.

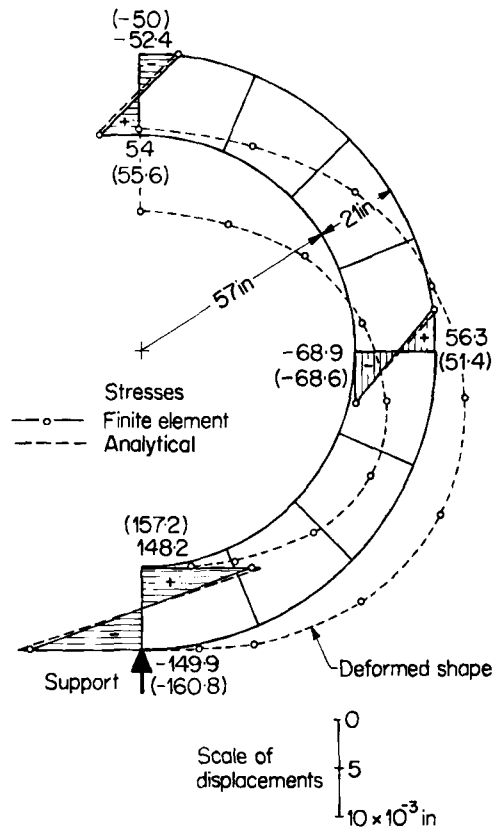

Figure 14. Long cylindrical shell under gravity action with line support—variation of hoop stresses and distortion of section. $E = 3 \times 10^6$ lb/in^2; $\nu = 0{\cdot}15$; $\gamma = 140$ lb/ft^3

Example 8

Barrel vault, Figures 15–17. This typical problem in structural engineering is shown in Figure 15(a). The vault has no edge beam and is supported by a rigid diaphragm at each end.

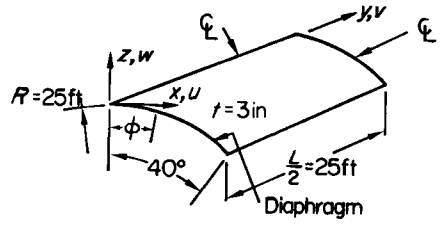

(a)

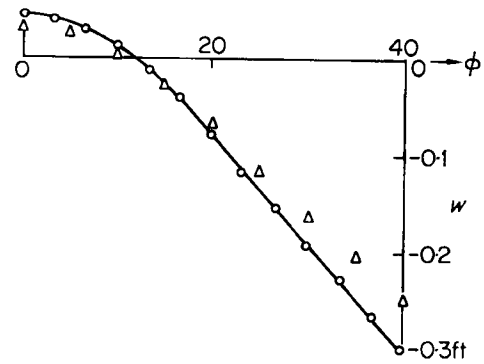

(b)

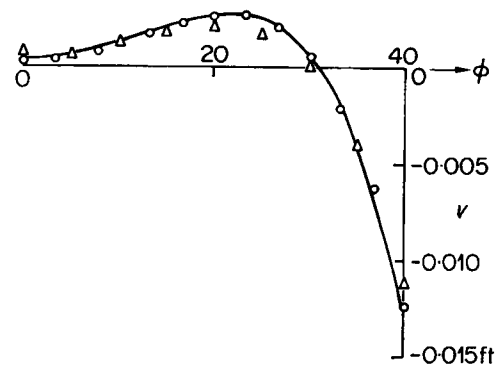

(c)

° 4×6 cubic elements
△ 4×6 parabolic elements
—— Exact

Figure 15. (a) Barrel vault. $E = 3 \times 10^6$ lb/in^2; $\nu = 0$; weight of shell = 90 lb/ft^2; (b) Vertical displacement (w) at central section, $y = L/2$; (c) Longitudinal displacement (v) at diaphragm, $y = 0$

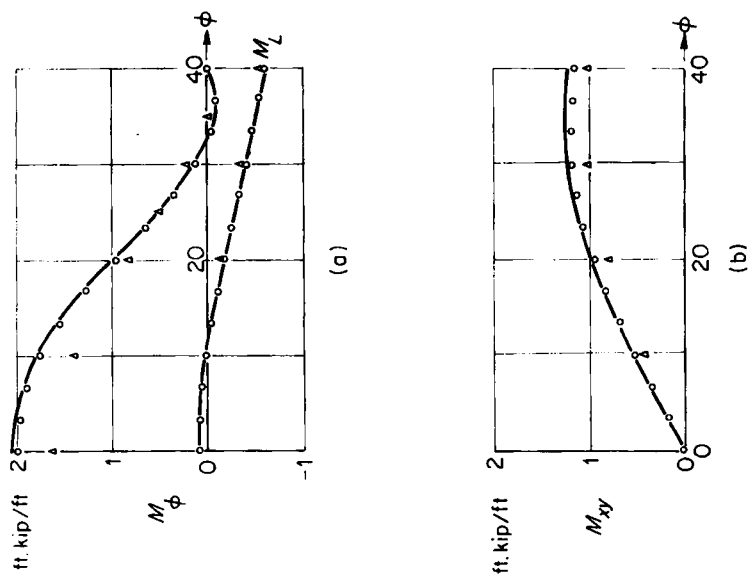

Figure 17. (a) Bending moments at central section, $y = L/2$. M_ϕ = Transverse moment; M_L = Longitudinal moment; (b) M_{xy} = Twisting moment at diaphragm

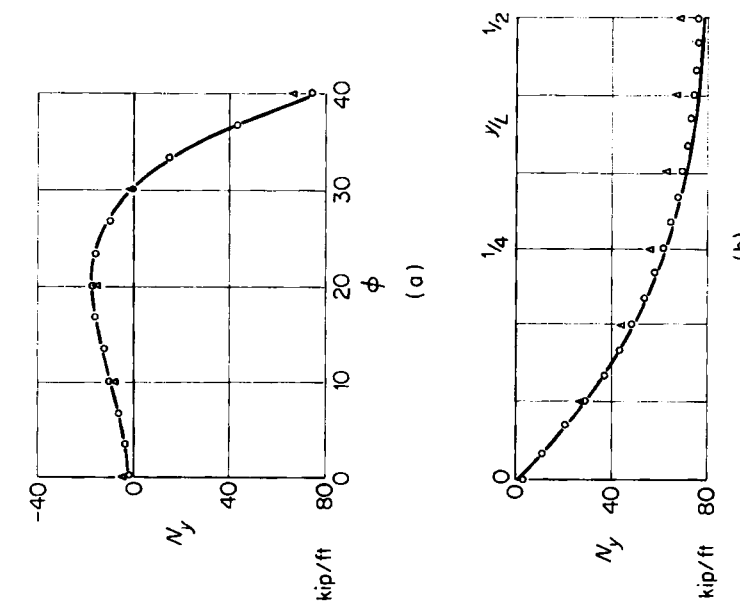

Figure 16. (a) Longitudinal force (N_y) at central section, $y = L/2$; (b) Longitudinal force (N_y) at free edge, $\phi = 40°$

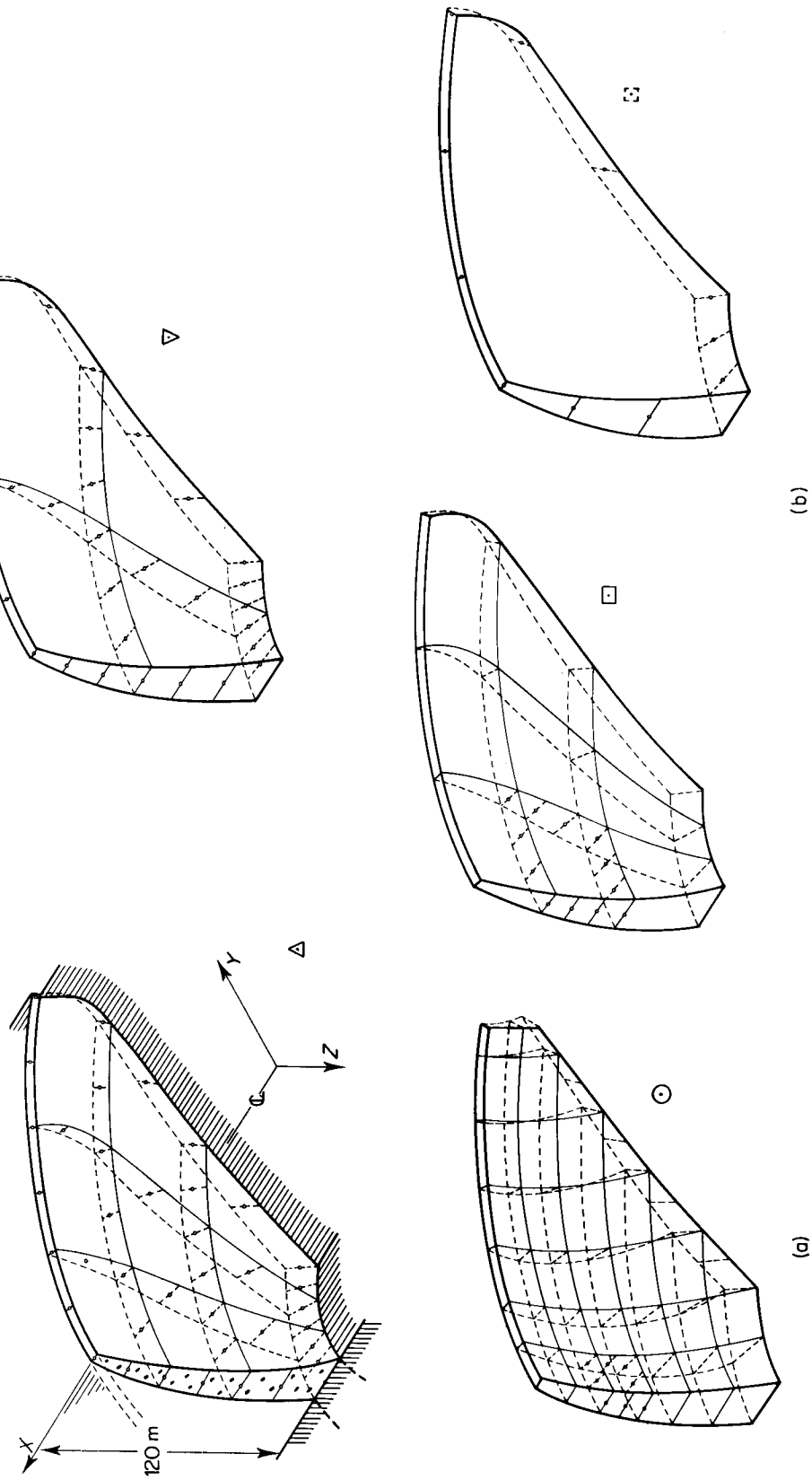

Figure 18. A doubly curved arch dam (Arch dam No. 5) in a 'rigid' valley; (a) Division into 9 and 32 parabolic elements; (b) Division into 4 and 9 cubic elements together with one-element representation. $E = 2 \times 10^5$ kg/cm^2; $\nu = 0{\cdot}15$

As the solution of this problem is known to involve appreciable bending stresses it provides a crucial test of large thin elements.

The figures show the improvement of accuracy when 24 cubic elements are used rather than 24 parabolic elements. This demonstrates once again the accuracy compared with an 'exact' solution.[23] The results compare favourably with a finite element solution obtained using flat triangular elements[3] and give better accuracy with fewer degrees of freedom.

Example 9

Arch dam with water load, Figures 18–21. The final example in this part is an arch dam, a thick shell structure with double curvature. The particular geometry, with rigid boundary conditions,

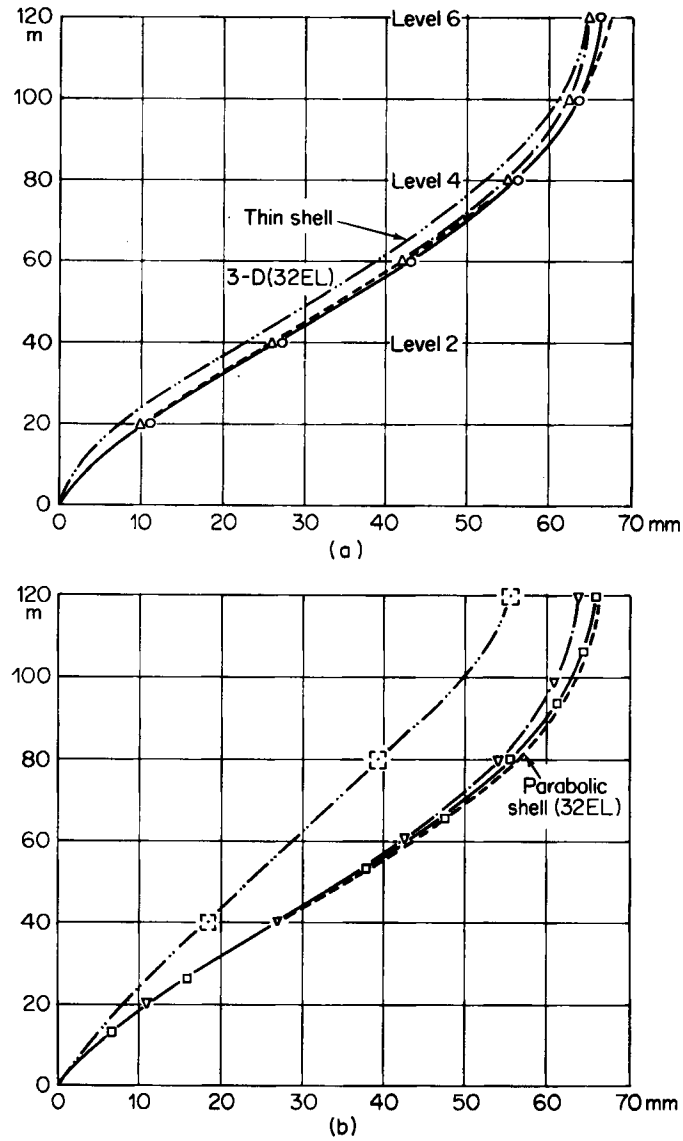

Figure 19. Downstream displacements ($-x$ direction) at the crown section; (a) Solution with parabolic elements; (b) Solution with cubic elements

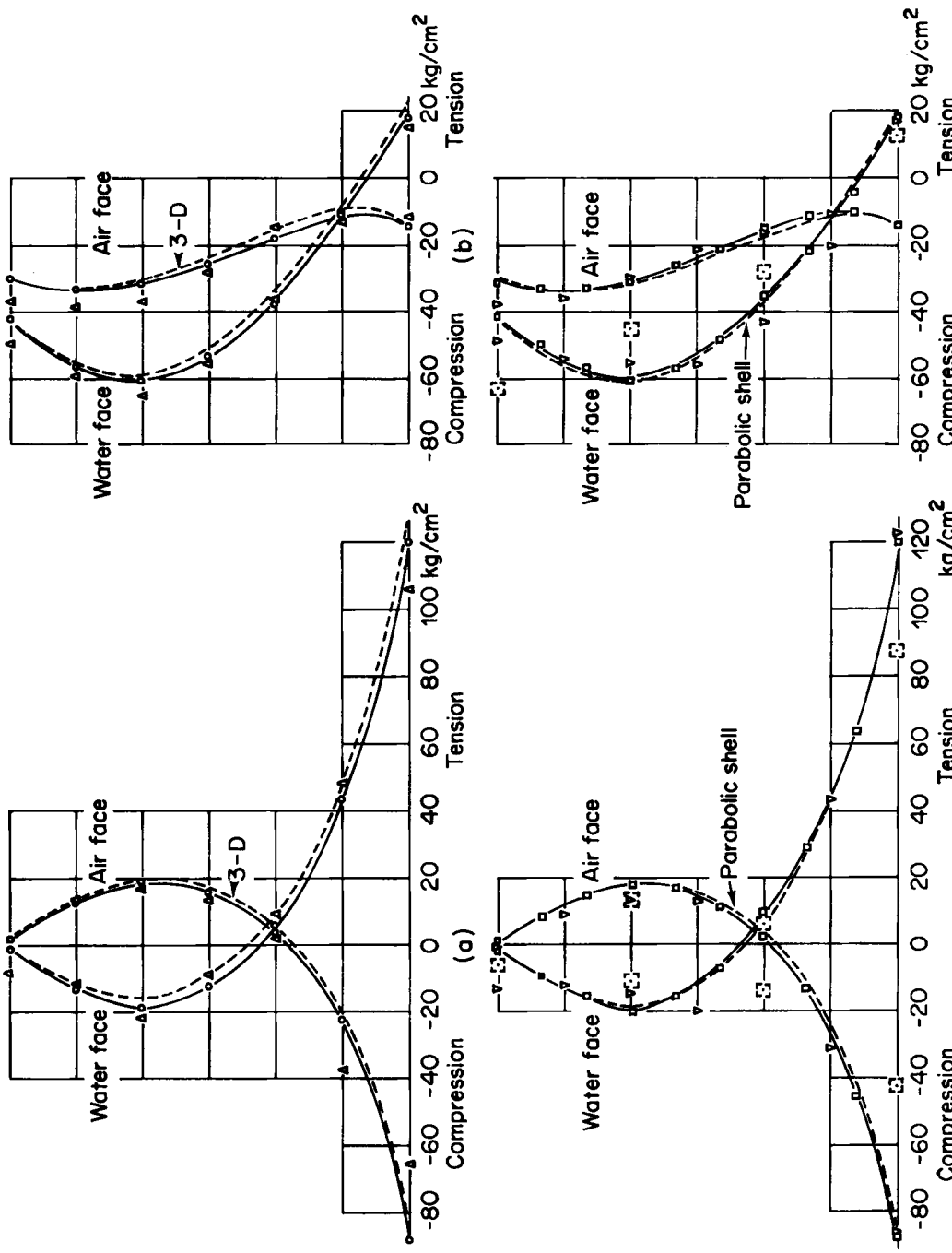

Figure 20. Stresses at the crown section; (a) Vertical stresses (σ_z) with parabolic elements; (b) Hoop stresses (σ_y) with parabolic elements; (c) Vertical stresses (σ_z) with cubic elements; (d) Hoop stresses (σ_y) with cubic elements

constituted a test problem (Arch dam No. 5) that was studied extensively by the Arch dams Committee of the Institution of Civil Engineers,[24] and for which many solutions were obtained using different methods. The most accurate results are presumably those attained by fully three-dimensional analysis, and hence the results given in Reference 11 are used for this comparison.

Figure 18 shows the various subdivisions used with parabolic and cubic elements and Figures 19 and 20 give various deflections and the stresses on centre-line. The agreement with the fully three-dimensional analysis with fine mesh using 32 parabolic elements is quite remarkable —indeed the slight increase in deflection probably results from shear warping ($k = 1{\cdot}2$) which is constrained in the three-dimensional case.

The saving in computation time is of the order of 40 per cent as fewer degrees of freedom are now required.

A closer examination of the stresses in Figures 20(a) and 20(b) will show that the curves due to three-dimensional analysis have slight additional tension everywhere. This is due to the difference in the nature of load application. In three-dimensional analysis the water pressure was replaced by pore pressure with the consequence of slightly upward pull.

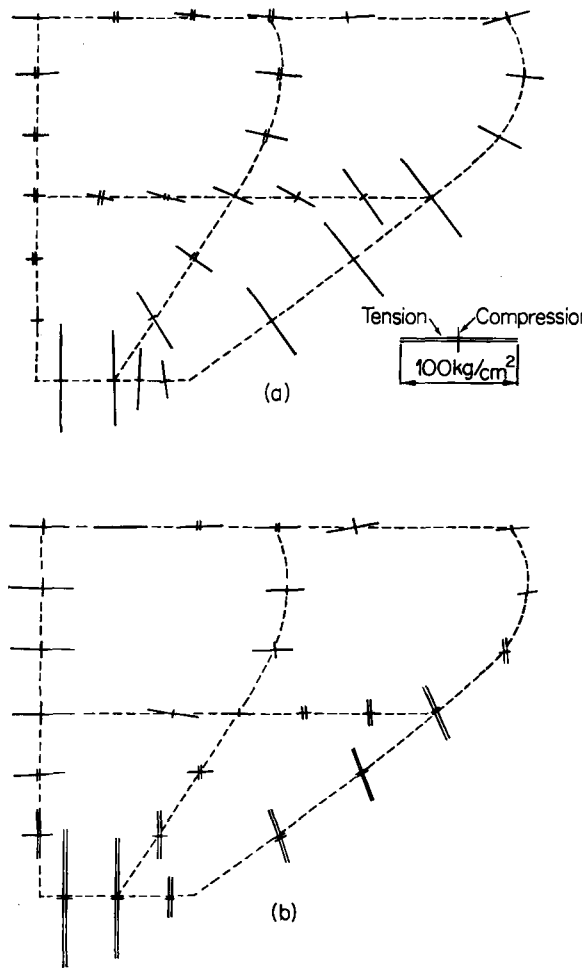

Figure 21. Principal stresses from the solution with four cubic elements; (a) Air face; (b) Water face

Thin shell solutions of the same problem give deflections some 3–4 per cent smaller,[2] indicating the effect of shear deformation.

However, the cubic shell element is even more promising. With only one cubic element (Figure 18b), the deflection is already 83 per cent of the best results. With only four cubic elements the results are acceptable (Figures 19 and 20). With nine cubic elements the deflections are within 1 per cent and the stresses show similar agreement. The number of degrees of freedom used with nine cubic elements and the time of computation is about two-thirds.

Figure 21 shows a plot of the principal stresses for the analysis with four cubic elements.

Clearly this example shows how the present program can deal effectively with such complex structures as arch dams of single or multiple vault configurations. For instance, a problem of a multiple vault structure shown in Figure 22 can readily be treated by the same process.

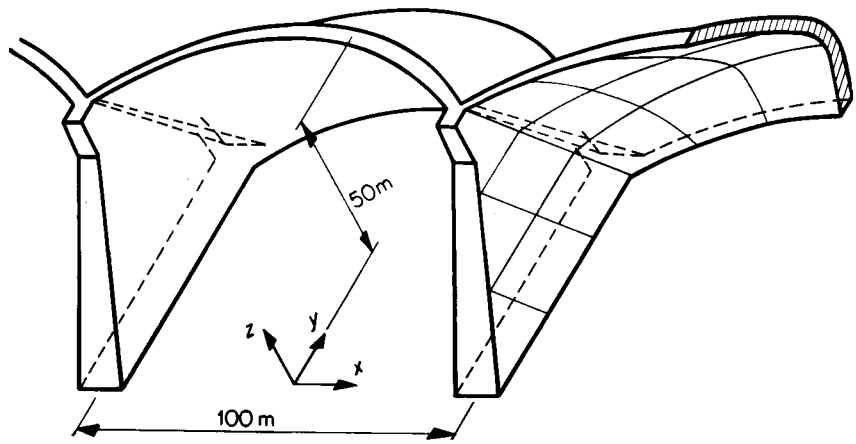

Figure 22. Multiple vault structure—subdivision into thick shell finite elements

ARCH DAMS WITH DEFORMABLE FOUNDATIONS

Deformable foundations

In the analysis of arch dams and indeed of other structures attached to a rock mass, significant deformations of the support will occur and these are often of paramount importance in the development of stresses in the shell. Indeed the mathematical fiction of unyielding, encastré supports is never realized in practice even in structurally simple situations (e.g. rotations of a concrete slab built into large supports of the same material will in general be so significant as to invalidate the results of a theoretically encastré analysis).

In three-dimensional analysis it is obviously possible to include the foundation continuum in the analysis.[11] In a shell-type approximation such treatment could again, in principle, be followed although difficulties of coupling this continuum to the shell would be experienced. As

(1) the structure is in general reasonably insensitive to the exact magnitude of the foundation stiffness, and

(2) the knowledge on rock deformability is at best approximate in a given situation,

a simpler procedure can be adopted.

In this the foundation stiffness is 'lumped' as a series of reaction coefficients. This process allows the solution to be obtained with exactly the same number of degrees of freedom as in the case of rigid foundations, permits an easy assessment of the effects of deformability coefficients and yields directly the total foundation forces. (These quantities are needed to consider the stability of the foundation.)

Vogt foundation parameters

The reaction of the shell on its foundation consists of five stress resultants, conveniently defined per unit length of foundation. Vogt[25] calculates the overall deformations of an elementary rectangle of length b in the direction of the shell on the basis of a semi-infinite elastic half-space using the well-known Boussinesq and Cerutti expressions. This type of calculation has for many years formed the basis of trial load analysis, and Reference 26 gives coefficients specifying the deformations, with some amendments listed in Reference 27.

Thus for a rectangular area on the side of the valley with local axes oriented as shown in Figure 23(a) the actions per unit length are direct forces F_x, F_y and F_z, a moment M_y and twisting couple M_z.

The corresponding average displacements of the rectangle (using the notation of Reference 27) are given by:

$$\begin{aligned} E_R u &= k_{\gamma'} F_x + \underline{k_{\alpha''} M_y/t} \\ E_R v &= k_{\gamma''} F_y \\ E_R w &= k_{\beta'} F_z \\ E_R \theta_y &= k_{\alpha'} M_y/t^2 + \underline{k_{\alpha''} F_x/t} \\ E_R \theta_z &= k_{\delta'} M_z/t^2 \end{aligned} \tag{18}$$

in which E_R is the modulus of the rock and the coefficients $k_{\gamma'}$, etc. depend on the Poisson's ratio and the proportion b/t.

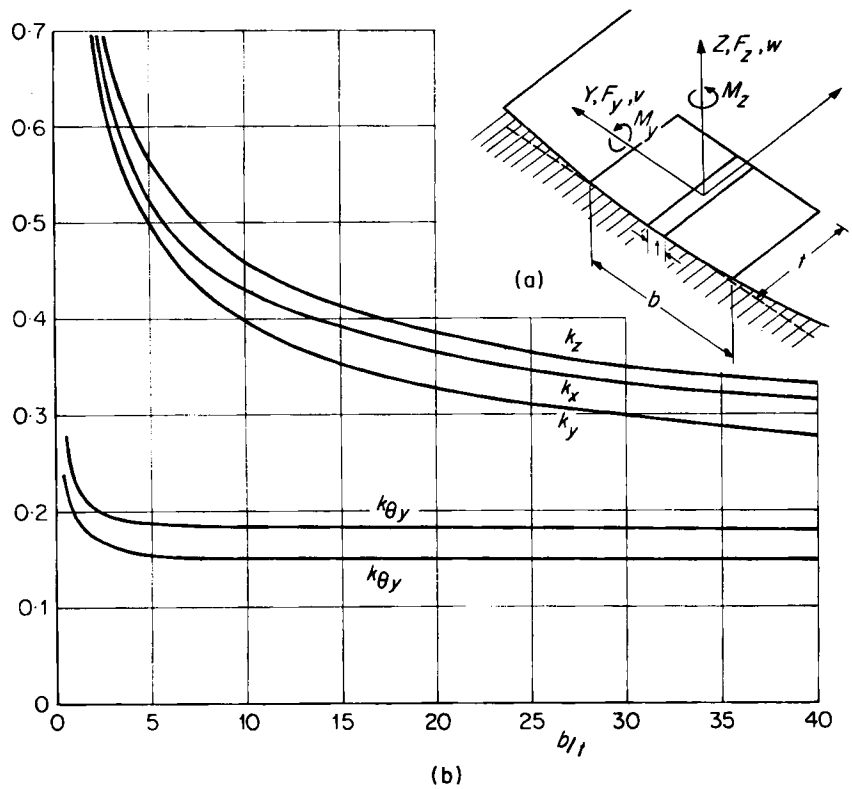

Figure 23. (a) Foundation strip with local axes; (b) Foundation stiffness coefficients (for $\nu = 0{\cdot}2$)

The underlined terms can be shown often to be small compared with the others and for simplicity will be omitted.

Equation (18) can now be rewritten in the form of a diagonal stiffness matrix assuming a length C to be contributory to the total nodal force.

$$C\begin{Bmatrix} F_x \\ F_y \\ F_z \\ M_y \\ M_z \end{Bmatrix} = CE_R \begin{bmatrix} k_x & & & & \\ & k_y & & 0 & \\ & & k_z & & \\ & & & k_{\theta y}t^2 & \\ & 0 & & & k_{\theta z}t^2 \end{bmatrix} \begin{Bmatrix} u \\ v \\ w \\ \theta_y \\ \theta_z \end{Bmatrix} \tag{19}$$

This matrix can be directly coupled to the shell analysis, noting appropriate direction changes. The stiffness coefficients, k_x, etc. are obtained from the corresponding values given in Reference 27 and are shown in Figure 23(b) for a Poisson ratio of 0·2 and various values of b/t.

In this type of analysis the cross coupling between adjacent nodes is neglected. Noting, however, that a real rock mass shows less cross coupling than would be indicated by an elastic continuum, the analysis provides a reasonable approximation.

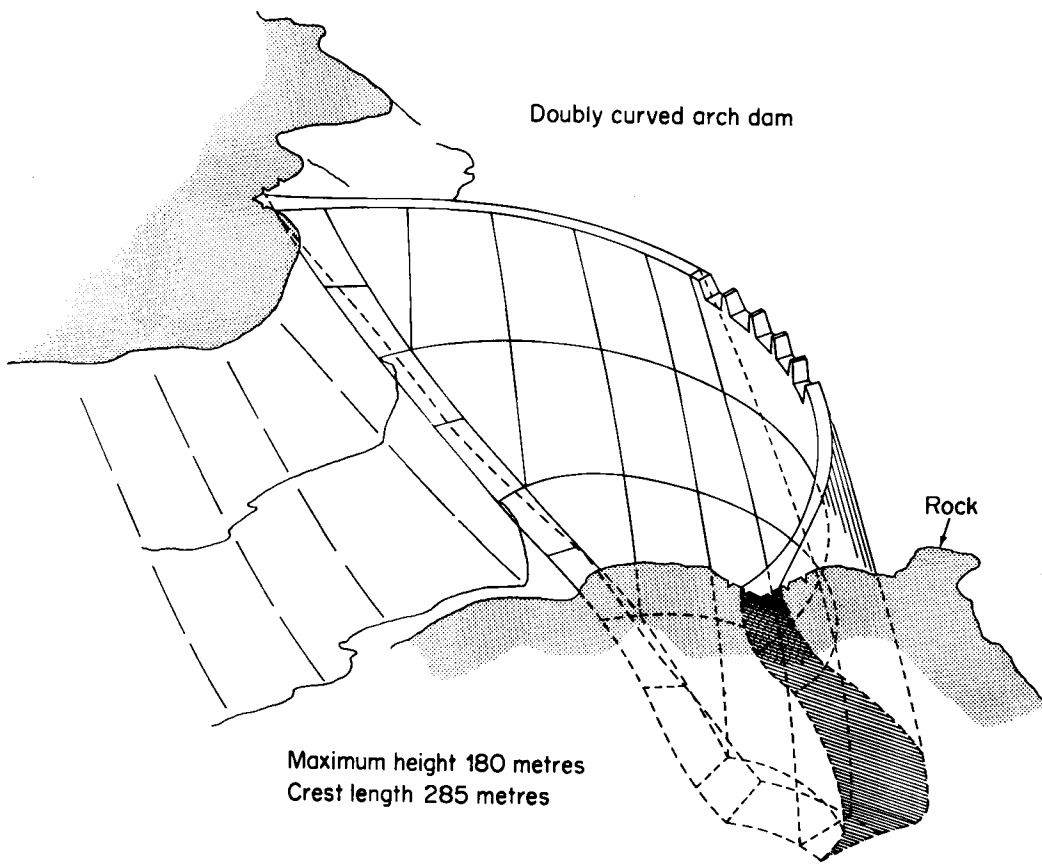

Figure 24. Doubly curved arch dam. Each half idealized with 23 parabolic elements

An alternative process has been suggested by Holand[28] who shows that the effect of the Vogt constants can be approximated by extending the shell by an amount l, with a new thickness t_0 and modulus E_0 given by

$$\left.\begin{aligned} l &= 0{\cdot}35t \\ t_0 &= 2{\cdot}3t \\ E_0 &= 0{\cdot}061E_R \end{aligned}\right\} \tag{20}$$

and fixing it rigidly beyond this limit. Because this treatment enlarges the problem the direct use of 'lumped' foundation stiffness is recommended.

A doubly curved arch dam

An analysis of a large arch dam, Figure 24, was recently conducted using a fully three-dimensional analysis and including an extensive foundation. The same dam was then reanalysed using

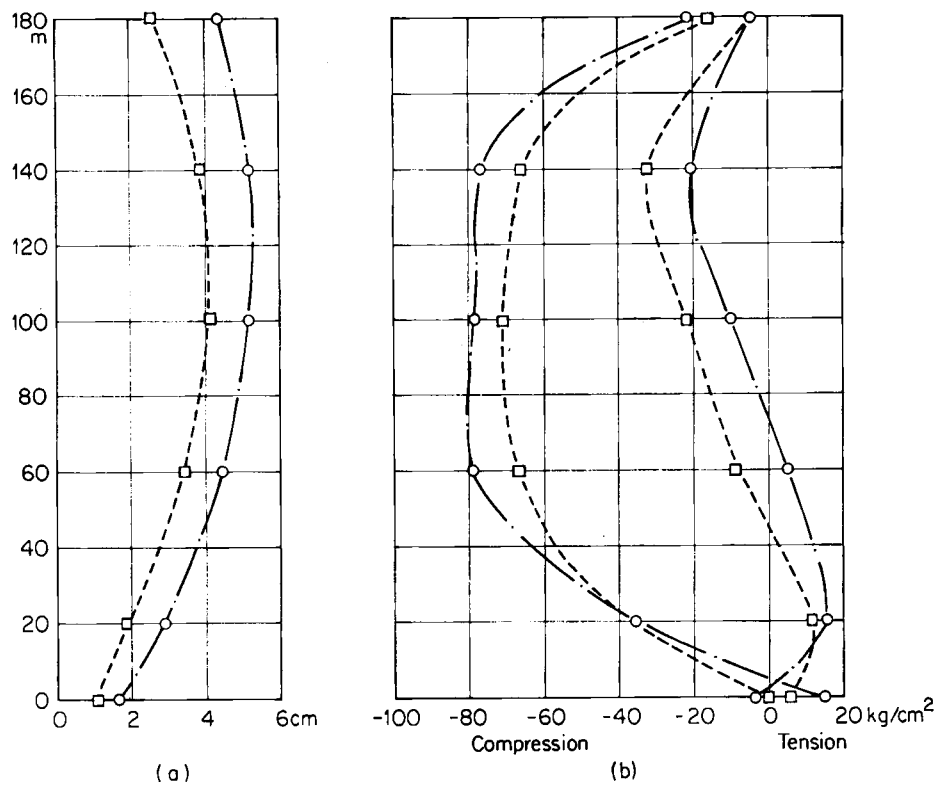

Figure 25. Analysis of a doubly curved arch dam with its foundation. $E = 2{\cdot}4 \times 10^5$ kg/cm^2; $\nu_{\text{concrete}} = 0{\cdot}15$; $\nu_{\text{rock}} = 0{\cdot}2$; (a) Downstream displacements of crown section; (b) Hoop stresses at the crown section. □ 3-D solution. ○ Thick shell solution.

present shell theory and lumped foundation parameters. Figures 25(a) and 25(b) compare the results. It will be noted that the deflection from shell analysis is slightly more than that obtained from three-dimensional analysis. This is due to the fact that in three-dimensional analysis only

one element was taken in the direction of the depth. A further subdivision of the foundation into finer elements would produce an increased deflection and consequently a closer agreement.

The lumping methods cannot reproduce foundation movements which may arise due to pore pressure action and in such cases the foundation movement must be independently estimated if the continuum is excluded from the analysis.

CONCLUSION

The examples shown illustrate the versatility and accuracy attainable with the new formulation. While less sophisticated approaches such as those presented in Reference 2 are by no means dispensed with (especially when the structural detail requires a very fine subdivision), the possibilities of curved element representation offer a tool generally more economical. An adequate representation of a complex situation by very few elements holds a promise of cheap and simple design modification and is an essential step in this computer-aided design process.

ACKNOWLEDGEMENTS

The authors would like to express their appreciation to the Science Research Council for sponsoring a part of this investigation and to 'Stressed Concrete Co. Ltd.' for permission to publish details of the hillside tank analysis.

APPENDIX I

Shape functions for elements of Figure 2(b)

Parabolic element:

Corner nodes $N_i = \frac{1}{4}(1+\xi_0)(1+\eta_0)(\xi_0+\eta_0-1)$

Mid-side nodes $(\xi_i = \pm 1, \eta_i = 0)$

$N_i = \frac{1}{2}(1+\xi_0)(1-\eta^2)$

with $\xi_0 = \xi . \xi_i$ and $\eta_0 = \eta . \eta_i$.

The other functions are deduced by interchanging ξ and η.

Cubic element:

Corner nodes $N_i = \frac{1}{32}(1+\xi_0)(1+\eta_0)\{-10+9(\xi^2+\eta^2)\}$

Mid-side nodes $(\xi = \pm 1, \eta_i = \pm \frac{1}{3})$

$N_i = \frac{9}{32}(1+\xi_0)(1-\eta^2)(1+9\eta_0)$, etc.

APPENDIX II

'Unique' definition of directions normal to a vector

If a vector $\vec{\mathbf{V}}_3$ is defined (by its three Cartesian components for instance) it is possible to erect an infinity of mutually perpendicular vectors orthogonal to it. Some scheme therefore has to be adopted to eliminate this choice—and indeed quite arbitrary decisions can be made here. A convenient scheme adopted in the present work related the choice to the global x or y axis.

If $\hat{\mathbf{i}}$ for instance is the unit vector along the x axis,

$$\vec{\mathbf{V}}_1 = \hat{\mathbf{i}} \times \vec{\mathbf{V}}_3$$

makes the vector $\vec{\mathbf{V}}_1$ perpendicular to the plane defined by the direction $\vec{\mathbf{V}}_3$ and the x axis.

As $\vec{\mathbf{V}}_2$ has to be orthogonal to both $\vec{\mathbf{V}}_3$ and $\vec{\mathbf{V}}_1$ we have

$$\vec{\mathbf{V}}_2 = \vec{\mathbf{V}}_3 \times \vec{\mathbf{V}}_1$$

To obtain unit vectors in the three directions $\vec{\mathbf{V}}_1$, $\vec{\mathbf{V}}_2$ and $\vec{\mathbf{V}}_3$ are simply divided by their scalar lengths, giving the unit vectors

$$\hat{\mathbf{v}}_1, \hat{\mathbf{v}}_2, \hat{\mathbf{v}}_3$$

On occasions the direction of the x axis and $\vec{\mathbf{V}}_3$ may coincide and this scheme breaks down. To avoid ambiguity the program checks for parallelism and in such cases starts with a unit vector $\hat{\mathbf{j}}$ along the y axis as an alternative in an identical set of operations.

APPENDIX III

Matrix handling scheme

A rudimentary matrix handling scheme proved invaluable in such matrix and vector operations in three-dimensional space.[14, 29] Out of an extensive set of operations, the general shell program used the scalar and vector products, a constant multiplied into a vector, a vector subtracted from another, the normalizing routine, matrix multiplication, matrix inversion, the two triple products and the 'Jacobi' eigenvalue routine (for principal stresses). For generality, the operations are performed in dynamic storage using the 3×83 array which also contains co-ordinates, etc.

APPENDIX IV

Notation

b = Length of rectangle in the direction of shell
$[\mathbf{B}']$ = Matrix connecting local strains to displacements
C = Contributory length
D = Diameter
$[\mathbf{D}']$ = Elasticity matrix in the local orthogonal system of co-ordinates
E = Young's modulus of elasticity in tension and compression
E_R = Young's modulus of elasticity of rock
E_0 = Modified Young's modulus
F_x, F_y, F_z = Direct forces per unit length in x, y and z directions respectively
i = Subscript indicating nodal number
$\hat{\mathbf{i}}, \hat{\mathbf{j}}$ = Vectors having unit values parallel to x and y axes respectively
$[\mathbf{J}]$ = Jacobian matrix
k = Constant factor included in $[\mathbf{D}']$ matrix to improve shear deformation
$k_x, k_y, k_z, k_{\theta y}, k_{\theta z}$ = Foundation stiffness coefficients
$k_{\gamma'}, k_{\gamma''}, k_{\beta'}, k_{\alpha'}, k_{\delta'}, k_{\alpha''}$ = Foundation flexibility coefficients
l = Extension of shell into foundation
M_y, M_z = Moments about y and z axes respectively
n = Harmonic number
N_i = A function of ξ, η taking a value of unity at the node i and zero at all other nodes
P_n = Amplitude of loading for nth harmonic
R = Radius

$[\mathbf{S}]$ = Matrix containing function of co-ordinates
t = Thickness
t_i = Thickness at node i
t_0 = Modified thickness
u, v, w = Components of displacements parallel to x, y and z axes respectively
u_i, v_i, w_i = Components of displacements at node i
$\hat{\mathbf{v}}_1, \hat{\mathbf{v}}_2, \hat{\mathbf{v}}_3$ = Unit vectors in x', y' and z' directions respectively
$\hat{\mathbf{v}}_{1i}, \hat{\mathbf{v}}_{2i}, \hat{\mathbf{v}}_{3i}$ = Unit vectors in x', y', z' directions at node i
$\vec{\mathbf{V}}_{3i}$ = Thickness vector at node i
x, y, z = Rectangular co-ordinates
x_i, y_i, z_i = Co-ordinates of node i
x', y', z' = Local system of rectangular co-ordinates
α, β = Rotations of nodal normal about two orthogonal axes
α_i, β_i = Rotation of normal at node i
$\gamma_{x'y'}, \gamma_{y'z'}, \gamma_{z'x'}$ = Shearing strain components in the local rectangular co-ordinates
$\{\boldsymbol{\delta}_i\}$ = Vector of displacement components at node i
$\{\boldsymbol{\delta}\}^e$ = Vector of nodal displacements of an element
$\{\boldsymbol{\varepsilon}'\}$ = Local strain vector
$\{\boldsymbol{\varepsilon}'_0\}$ = Local initial strain vector
$\varepsilon_{x'}, \varepsilon_{y'}$ = Strains in x' and y' directions respectively
ζ = A linear co-ordinate in the thickness direction
ζ_i = ζ-co-ordinate at node i
η, ξ = Curvilinear co-ordinates in the plane of the shell
η_i, ξ_i = η, ξ co-ordinates at node i
θ = Angular co-ordinate in the circumferential direction
$[\boldsymbol{\theta}]$ = Direction cosine matrix of a local orthogonal system of axes
θ_y, θ_z = Rotations about y and z axes respectively
ν = Poisson's ratio
$\sigma_{x'}, \sigma_{y'}$ = Normal stress components parallel to x' and y' axes respectively
$\tau_{x'y'}, \tau_{y'z'}, \tau_{z'x'}$ = Shearing stress components in the local rectangular co-ordinates
$\sum$ = Summation
$\int$ = Integral

REFERENCES

1. O. C. Zienkiewicz and Y. K. Cheung, *The Finite Element Method in Structural and Continuum Mechanics*, McGraw–Hill, London and New York, 1967.
2. O. C. Zienkiewicz, C. Parekh and I. P. King, 'Arch dams analysed by a linear finite element shell solution program', *Proc. Symp. Arch dams, Inst. civ. Engrs, London*, 19–22 (1968).
3. R. W. Clough and C. P. Johnson, 'A finite element approximation for the analysis of thin shells', *Int. J. Solids Structures*, **4**, 43–60 (1968).
4. G. E. Strickland and W. A. Loden, 'A doubly-curved triangular shell element', *Proc. Conf. Matrix Meth. Struct. Mech. Wright–Patterson Air Force Base, Ohio*, AFFDL-TR-68-150, 641–666 (1968).
5. B. E. Greene, R. E. Jones, R. W. McLay and D. R. Strome, 'Dynamic analysis of shells using doubly curved finite elements', *Proc. Conf. Matrix Meth. Struct. Mech. Wright–Patterson Air Force Base, Ohio*, AFFDL-TR-68-150, 185–212 (1968).
6. J. J. Connor and C. Brebbia, 'Stiffness matrix for shallow rectangular shell element', *J. Engng Mech. Div. Am. Soc. civ. Engrs*, **93**, EM5, 5528, 43–65 (1967).
7. S. Utku, 'Stiffness matrices for thin triangular elements of nonzero Gaussian curvature', *AIAA Jnl*, **5**, 9, 1659–1667 (1967).

8. B. M. Irons, 'Engineering application of numerical integration in stiffness methods', *AIAA Jnl*, **4**, 11, 2035–2037 (1966).
9. J. Ergatoudis, B. M. Irons and O. C. Zienkiewicz, 'Three-dimensional stress analysis of arch dams by the finite element method': Part I, Arch dam No. 1, October 1966; Part II, Arch dam No. 5, December 1966, AD/1735 and AD/1745, Reports to Arch dams Committee of Institute of Civil Engineers, London, 1966, Research Report No. C.R58/66 University of Wales, Swansea.
10. J. Ergatoudis, B. M. Irons and O. C. Zienkiewicz, 'Curved isoparametric quadrilateral elements for finite element analysis', *Int. J. Solids Structures*, **4**, 31–42 (1968).
11. J. Ergatoudis, B. M. Irons and O. C. Zienkiewicz, 'Three-dimensional stress analysis of arch dams and their foundations', *Proc. Symp. Arch amsd, Inst. civ. Engrs, London*, 37–50 (1968).
12. S. Ahmad, B. M. Irons and O. C. Zienkiewicz, 'Curved thick shell and membrane elements with particular reference to axi-symmetric problems', *Proc. Conf. Matrix Meth. Struct. Mech. Wright–Patterson Air Force Base, Ohio*, AFFDL-TR-68-150, 539–572 (1968).
13. B. M. Irons, 'A frontal solution program for finite element analysis', *Int. J. num. Meth. Engng*, **2**, 1, 5–32 (1970).
14. S. Ahmad, *Curved Finite Elements in the Analysis of Solid, Shell and Plate Structures*, Ph.D. Thesis, University of Wales, Swansea, Appendix 2, 1969, pp. 158–173.
15. S. Timoshenko and S. Woinowsky-Krieger, *Theory of Plates and Shells*, 2nd edn., McGraw–Hill, New York, 1959.
16. P. E. Grafton and D. R. Strome, 'Analysis of axi-symmetric shells by the direct stiffness method', *AIAA Jnl*, **1**, 2342–2347 (1963).
17. J. H. Percy, T. H. H. Pian, S. K. Klein and D. R. Navaratna, 'Application of matrix displacement method to linear elastic analysis of shells of revolution', *AIAA Jnl*, **3**, 2138–2145 (1965).
18. J. Ergatoudis, *Isoparametric Finite Elements in Two- and Three-dimensional Analysis*, Ph.D. Thesis, University of Wales, Swansea, 1968.
19. E. L. Albasiny and D. W. Martin, 'Bending and membrane equilibrium in cooling towers', *J. Engng Mech. Div. Am. Soc. civ. Engrs*, EM3, 5256, 1–17 (1967).
20. E. Reissner, 'The effect of transverse shear deformation on the bending of elastic plates', *J. Appl. Mech.*, **12**, A69–A77 (1945).
21. Y. K. Cheung, I. P. King and O. C. Zienkiewicz, 'Slab bridges and arbitrary shape and support conditions: a general method of analysis based on finite elements', *Proc. Inst. civ. Engrs*, **40**, 9–36 (1968).
22. S. Timoshenko, *Strength of Materials, Part II*, 3rd edn., Van Nostrand, New York, 1956, pp. 96–101.
23. A. C. Scordelis and K. S. Lo, 'Computer analysis of cylindrical shells', *J. Am. Concr. Inst.*, **61**, 1, 539–561 (1964).
24. *Arch dams: a Review of British Research and Development, Inst. civ. Engrs, London*, 1968, pp. 37–50.
25. F. Vogt, *Über die Berechnung der Fundament Deformation*, Der Norske Videnkops Akaemi, Oslo, 1925.
26. *Trial Load Method of Analysing Arch dams*, United States Bureau of Reclamation, Boulder Canyon Project, Part V, Bulletin 1, 1938.
27. V. Mladyenovitch, 'Déformations des fondations de barrages', *Travaux*, **6**, 3–15 (1966).
28. I. Holand, 'Incorporation of foundation deformation in a finite element shell analysis', *Proc. Symp. Arch dams, Inst. civ. Engrs, London*, 1968.
29. S. Ahmad, B. M. Irons and O. C. Zienkiewicz, 'A simple matrix-vector handling scheme for 3-D and shell analysis', *Int. J. num. Meth. Engng.* (to be published).